RM L50K27

NACA

RESEARCH MEMORANDUM

AN EXPERIMENTAL STUDY AT MODERATE AND HIGH SUBSONIC SPEEDS OF THE FLOW OVER WINGS WITH 30° AND 45° OF SWEEPBACK IN CONJUNCTION WITH A FUSELAGE

By Richard T. Whitcomb

Langley Aeronautical Laboratory
Langley Field, Va.

NATIONAL ADVISORY COMMITTEE
FOR AERONAUTICS

WASHINGTON
June 15, 1951

NATIONAL ADVISORY COMMITTEE FOR AERONAUTICS

RESEARCH MEMORANDUM

AN EXPERIMENTAL STUDY AT MODERATE AND HIGH SUBSONIC SPEEDS OF THE FLOW OVER WINGS WITH 30° AND 45° OF SWEEPBACK IN CONJUNCTION WITH A FUSELAGE

By Richard T. Whitcomb

SUMMARY

Pressure distributions, wake measurements, and tuft patterns have been obtained for wings with 30° and 45° of sweepback in conjunction with a midwing fuselage at Mach numbers to 0.96. The wings have an NACA 65-210 section, a taper ratio of 2.6:1, and aspect ratios of 7.5 and 5.2. A study of the results of these measurements indicates that, when the Mach number was increased to high subsonic values at low angles of attack, the locations of the peak negative pressure coefficients on the upper surfaces of sections near the wing-fuselage junctures shifted rearward markedly. Some reduction of the profile-drag coefficient with increasing sweep at subcritical Mach numbers was indicated.

For the wing with 30° of sweepback at low angles of attack, separation associated with onset of shock occurred initially on the midsemispan region of the upper surface. When the Mach number was increased to values considerably above the drag-divergence value, the region of most severe separation spread outward. At Mach numbers up to 0.925, no perceptible separation was observed near the wing-fuselage juncture on the upper surface of the wing with 30° of sweepback at all high angles of attack, in spite of the fact that strong shocks were present above this region for some conditions. Generally, the spanwise pressure gradients on sweptback wings resulted in reductions of the boundary-layer separation on the inboard section and aggravations of separation on the outboard sections.

INTRODUCTION

In order to provide a basis for a further understanding of the flow over unswept and swept wings at high subsonic speeds, pressure,

tuft, and wake measurements have been made on and behind a high-aspect-ratio tapered wing with 0° sweep and with 30° and 45° of sweepback and sweepforward in conjunction with a typical fuselage. These measurements were made in the Langley 8-foot high-speed tunnel at Mach numbers from 0.60 to 0.96. A relatively extensive study of the measurements made for the sweptback wings is presented herein. Similar studies for the unswept and sweptforward wings are presented in references 1 and 2.

SYMBOLS

b	span of model
d	sweptback semispan, distance between intersections of quarter-chord line (said chords perpendicular to this line) with root and tip sections parallel with air stream
s	distance measured along quarter-chord line from plane of symmetry
c_Λ	section chord perpendicular to quarter-chord line
$\bar{c}_w$	mean aerodynamic chord of wing in stream direction (fig. 1)
l	distance from leading edge of wing perpendicular to quarter-chord line
Λ	sweep angle between line perpendicular to plane of symmetry and quarter-chord line
α	geometric angle of attack
M	Mach number
q	dynamic pressure in undisturbed stream, pounds per square foot $\left(\frac{1}{2}\rho V^2\right)$
V	velocity in undisturbed stream, feet per second
ρ	mass density in undisturbed stream, slugs per cubic foot
p	local static pressure at a point on airfoil or fuselage, pounds per square foot

p_o static pressure in undisturbed stream, pounds per square foot

P pressure coefficient $\left(\frac{p - p_o}{q}\right)$

c_n wing-section normal-force coefficient (section perpendicular to quarter-chord line) $\left(\frac{1}{c_\Lambda}\int_0^{c_\Lambda}\left(P_L - P_U\right)dl\right)$

c_{d_o} indicated wing-section profile-drag coefficient from wake-survey measurements based on local chord in stream direction

ΔH total-pressure loss, pounds per square foot

Subscripts:

L lower surface

U upper surface

cr critical

APPARATUS

Wing models.- The models tested to obtain the results for the unswept wing as described in reference 1 were also used to obtain the data for the sweptback configurations as presented herein. For the unswept condition, the configuration investigated has an NACA 65-210 section, an aspect ratio of 9.0, and a taper ratio of 0.4, with no twist or dihedral. The models were supported in the tunnel by means of the vertical steel plate which is completely described in reference 3. Swept configurations were obtained by rotating the complete wings with respect to the fixed support plate. Wall-pressure measurements indicate that the flow over the model on one side of the plate had very little effect on the flow on the other side even at the highest test Mach numbers. A given configuration represents, therefore, not a yawed model but half a sweptback model and half a sweptforward model. Plan forms and basic dimensions of the configurations with 30° and 45° of sweepback are presented in figure 1. The aspect ratios for the two wings are 7.5 and 5.2; the taper ratios are 0.38. Detailed dimensions are given in table I of reference 4.

Two wing models were used in the investigation. One, used to obtain the static-pressure data, incorporated 20 static-pressure orifices at each of eight stations along the wing semispan in lines perpendicular to the quarter-chord line. The locations of the orifices are presented in reference 5. A 20-percent-chord, straight-sided aileron as shown in figure 1 was incorporated in this model. The angle of the aileron was 0° for the investigation reported herein. The second wing model, used for the wake and tuft measurements, incorporated no pressure orifices or aileron.

Fuselage.- The fuselage was simulated by the addition of two half bodies of revolution to the test configuration at the surface of the support plate. The dimensions of the half bodies of revolution, the center lines of which coincided with the chord plane of the wing, are presented in reference 4. Twenty-eight pressure orifices were placed in one of the halves of the fuselage in two planes at 45° to the plane of symmetry through the center line, as shown in figure 1.

Survey apparatus.- Total- and static-pressure measurements were made at various vertical stations behind the wing by means of the rake shown with the unswept configuration in figure 2 and described in reference 4. Tuft surveys were made with tufts of fine woven nylon line which were fastened to the surface of the wing and fuselage of the configurations with cellulose cement.

Reynolds numbers.- The variations of Reynolds number with Mach number for the configurations with the two angles of sweepback are presented in figure 3. The Reynolds numbers are based on the mean aerodynamic chord of the wings outboard of the fuselage.

RESULTS

Pressure distributions.- The distributions of pressure on the wings with 30° and 45° of sweepback for a number of test conditions are presented in figures 4 and 5, respectively. Other pressure data obtained during the investigation are presented in reference 3. The distributions are presented in the form of contours of equal pressure coefficient on plan forms of the wing. The positions of the chordwise pressure peaks are indicated by lines of short dashes. The locations of the rows of pressure orifices and the tenths of chords of the various stations are indicated by light lines of long dashes. In order to indicate more explicitly the changes in pressure on the wings near the wing-fuselage juncture, pressure distributions in the stream direction at a station 0.25-fuselage radius from the surface of the fuselage obtained from the pressure contours are presented in figures 6 and 7. Spanwise variations in wing section normal-force coefficient c_n are presented in figures 8

and 9. The coefficients presented are for sections perpendicular to the quarter-chord line.

Tuft patterns and wake measurements.- Selected tuft patterns obtained on the upper and lower surfaces of the configurations are presented in figures 10 and 11.

Some of the distributions of total-pressure loss in planes parallel to the plane of symmetry at various measurement stations behind the wings are presented in figures 12 and 13. The spanwise variations of indicated wing section profile-drag coefficient for various Mach numbers at several angles of attack are presented in figures 14 and 15. These coefficients were obtained from the total-pressure measurements by use of the method described in reference 6. The wake measurements were made at stations shown in figure 1 and listed in reference 5. The total-pressure data presented for the wing with 45° of sweepback at an angle of attack of 2° were obtained by interpolating between the results obtained at 0° and 3° angle of attack. No total-pressure measurements were made behind the fuselage, so that a complete indication of the spanwise variation of profile drag cannot be presented.

Corrections.- No corrections for the effects of tunnel-wall interference have been applied to the data presented. Estimations of the order of magnitude of these effects indicate that the corrections to be applied to dynamic pressures and Mach numbers for all conditions are less, and in most cases much less, than 1 percent. Only data relatively free from choking effects have been used in this study. A discussion of the limitations imposed by blockage interference near choking during the investigation is presented in reference 4. The results of calculations of the bending of the wing produced by the air loads on the structure similar to those described in reference 7 indicate that this bending results in tip washout for all conditions. The maximum reductions of the aerodynamic angles of attack, at a Mach number of 0.96 for the wing with 45° of sweepback, are approximately 10 percent of the mean aerodynamic angles of attack for the wing. Such reductions should not generally result in significant changes in the flow phenomena discussed herein.

DISCUSSION

Angle of Attack of 2° at a Subcritical Mach Number of 0.60

Pressure distributions.- At an angle of attack of 2° for a Mach number of 0.60, the induced velocities along the midchord regions of the upper surfaces of the wing-fuselage-juncture sections of the wings are less than those on the corresponding regions of sections farther outboard for which measurements are available (figs. 4(a) and 5(a)). Part of this difference is due to the induced flow associated with the swept wings.

However, the major portion of the reduction is believed to be due to the effect of the fuselage, as was a similar variation for the comparable unswept wing (fig. 16 and reference 1). Small local-pressure peaks are present near the leading edge of the upper surface of the wing with 30° of sweepback at the juncture of the wing and fuselage, as on the unswept wing. The peak on the wing with 30° of sweep is considerably less pronounced than that on the unswept wing while no peak is present on the wing with 45° of sweep. Thus the magnitude of the peak decreases with sweep.

Boundary-layer flow.- The wake measurements indicate that at a Mach number of 0.60 and at angles of attack of 0° and 2° the profile-drag coefficients for the various wing sections decrease with increasing sweepback (figs. 14 and 15). As a result, the over-all profile-drag coefficients decrease (fig. 17). Similar reductions in the profile-drag coefficient associated with sweepback are indicated by data obtained at the same Mach number and at relatively high Reynolds numbers (reference 8) in the Langley 16-foot high-speed tunnel for a wing with an NACA 65-215 section and with the same sweeps as those of the present configurations. These reductions may be attributed primarily to reductions in the local induced velocities resulting from sweep. Among other factors, it may be due to an extension of the laminar boundary layer associated with the reduction in Reynolds number based on the component of velocity normal to the leading edge.

The indicated profile-drag coefficients for sections of the swept-back wings generally increase from root to tip. These variations might be attributed to a slight outward spanwise flow in the boundary layer and to the spanwise variations of the Reynolds number and the chordwise extent of favorable streamwise pressure gradients.

Angle of Attack of 2° at a Mach Number Slightly Below the Drag-Divergence Value

The drag-divergence Mach numbers for the wings with 0°, 30°, and 45° of sweep are approximately 0.74, 0.83, and 0.93 (fig. 17). (The delay in the drag rise produced by 30° of sweepback is approximately 80 percent of that predicted using the simple sweep theory; that produced by 45° of sweepback is approximately 60 percent of the predicted value.)

Pressure distributions.- When the Mach numbers are increased from 0.6 to 0.80 and 0.89 for the wings with 30° and 45° of sweep, respectively, (figs. 4 and 5), the negative pressure coefficients on the upper surface of sections near the wing-fuselage juncture decrease over the forward portion of the chord and increase over the rearward portion (figs. 6 and 7). As a result, the peaks on these sections move aft by considerable

amounts. Generally, these changes in the pressure coefficients are quite similar to those that occur on an unswept surface at supercritical Mach numbers when no separation is present, although they are not caused by the same phenomena. This effect is not caused by the presence of the fuselage. Similar changes are indicated by data obtained during other investigations of similar sweptback wings at high subsonic Mach numbers, for which no fuselages were present (references 9 and 10, for example). Such changes in the pressure distributions at these Mach numbers are qualitatively similar to those predicted by the linear theory for nonlifting surfaces (reference 11).

The negative pressure peak near the leading edges of the sections of the wing with 30° of sweep near the wing-fuselage junctures at a Mach number of 0.60 disappears when the Mach number is increased to 0.80.

When the Mach numbers are increased from 0.60 to 0.80 and 0.89 for the wings with 30° and 45° of sweepback, respectively, the negative pressure coefficients near the leading edges of sections near the tip increase instead of decreasing, as they do on the corresponding regions of the midsemispan sections; near the trailing edges of these sections, the negative pressure coefficients decrease instead of remaining approximately constant as they do on the aft portions of the midsemispan sections. Such variations are predicted by the theory presented in reference 11.

Definite streamwise retarding pressure forces act on the sections of the wing near the junctures at the conditions under consideration, because of the forms of the pressure distributions on these regions. No energy loss, and therefore no drag, is associated with these retarding forces (figs. 12 and 13). The retarding forces are balanced by streamwise accelerating forces acting on the sections farther outboard. This balancing of streamwise forces is mentioned in reference 11.

When the Mach numbers are increased to the values under consideration, the critical Mach numbers on the upper surfaces at all spanwise stations of these two wings are exceeded (figs. 4(b) and 5(b)). Because of the effects of sweep, no perceptible shocks or separation are associated with these supersonic local Mach numbers.

Angle of Attack of 2° at Mach Numbers Slightly Greater Than the Drag-Divergence Values

Data obtained at Mach numbers of 0.85 and 0.96 for the wings with 30° and 45° of sweepback, respectively, provide an indication of the nature of the flow over sweptback wings at Mach numbers slightly greater than the drag-divergence values (fig. 17).

Pressure distributions.- When the Mach numbers are increased to 0.85 and 0.96 for the wings with 30° and 45° of sweepback, respectively, the chordwise pressure distributions on the midsemispan region of the upper surfaces of the sweptback wings (figs. 4 and 5) change approximately as they do on the unswept wing in this region at a nearly comparable Mach number of 0.80 (fig. 16). Near the wing-fuselage juncture, the pressure distributions on the upper surfaces continue to change as they do at Mach numbers below the drag-divergence values. For sections near the juncture, the maximum induced velocities on the upper surface are believed to be reduced by the presence of the fuselage, as they are at lower speeds.

At Mach numbers above the drag-divergence values, the angles of obliqueness of the lines of maximum induced velocities at the various sections of the wings are considerably less than the nominal sweep angles. At Mach numbers of 0.85 and 0.96 for the wings with 30° and 45° of sweepback, the angles of these lines with respect to the normal to the stream are approximately 0° near the juncture, 27° and 39° in the midsemispan region, and 19° and 24° near the tip. Similar variations have been measured on a wing with 35° of sweep at comparable conditions (reference 10).

In an attempt to provide some logical basis for correlating the results of the pressure measurements with those of the wake and tuft surveys, it has been assumed that the strengths of the shocks on the various sections of the wings are functions of the components of the actual maximum Mach numbers normal to the lines of maximum negative pressure (figs. 4 and 5). Calculations indicate that for each of the wings, at the conditions under consideration, these Mach number components on the upper surfaces of the various sections are approximately the same, being about 1.17 for each of the sections of the wing with 30° of sweepback and 1.14 for those of the wing with 45° of sweep. In computing these Mach number components, it has been assumed that the lateral deflections of the streamlines on the outboard regions are equal to those of infinite-span surfaces with the same pressure distributions as those measured. It was assumed that no cross flow existed on the juncture section.

Shocks.- The forms of the chordwise pressure distributions on the wings indicate that shocks may be associated with the supersonic local effective maximum velocities on the upper surfaces of the various sections of the wings at the Mach numbers slightly above the drag-divergence values (figs. 4(d) and 5(c)). (The presence of shocks is indicated by the severe adverse chordwise pressure gradients downstream of the region of maximum induced velocities.) However, the losses in these shocks are not perceptible by the available wake measurements.

Boundary-layer flow.- The tuft patterns obtained on the upper surface of the wing with 30° of sweepback for an angle of attack of 2° at a Mach number of 0.85 (fig. 10(d)) indicate that, for this angle of attack, the initial increase in boundary-layer losses associated with onset of shock probably occurs at about the midchord station of the mid-semispan section. (The increase in boundary-layer losses due to shock on a sweptback wing at low angles of attack is generally indicated by an abrupt redirection of the tufts outward.) The largest relative amount of low-energy air (fig. 14) associated with the separation on the upper surface leaves the trailing edge somewhat outboard of the station at which the maximum energy loss is indicated by the tufts. This phenomenon is probably a result of the outward flow of the low-energy air on the wing surface associated with the spanwise pressure gradients.

Both the tuft patterns and wake measurements indicate that there is little separation on the wing with 30° of sweepback near the wing-fuselage juncture or near the tip at a Mach number of 0.85, even though it appears that the shock is present above these sections.

Angle of Attack of 2° at Mach Numbers Considerably Higher Than the Drag-Divergence Value for the Wing with 30° of Sweepback

Because of the limitation of the tunnel speed, no data were obtained for the wing with 45° of sweepback for Mach numbers greater than that for drag divergence at 2° angle of attack.

Pressure distributions.- When the Mach number is increased from 0.85 to 0.96 for the wing with 30° of sweepback at an angle of attack of 2°, the shapes of the chordwise pressure distributions on the upper surface generally continue to change as they do when the Mach number is increased beyond the drag-divergence value (figs. 4 and 6).

When the Mach number is increased from 0.89 to 0.96, a perceptible change occurs in the magnitude and distribution of pressures on the various sections of the lower surface (fig. 4). These changes are similar to the variations that occur on the unswept wing at the comparable Mach number of 0.89 (reference 1).

For the wing with 30° of sweepback at a Mach number of 0.89, the effective maximum local Mach numbers are approximately the same at each of the various sections, as they are at lower speeds. The maximum Mach number is about 1.33.

Shocks.- When the Mach number is increased from 0.85 to 0.89, the losses due to the shock on the upper surface of the wing with 30° of sweepback become perceptible by the wake measurements made at all spanwise stations (fig. 12(a)). (Although the wake measurements do not indicate accurately the spanwise location of the origin of boundary-layer losses on sweptback wings, they do reveal fairly reliably the spanwise variations of shock losses for these wings.) The shock is relatively weak and has approximately the same strength above the various stations.

The relatively severe total-pressure losses measured approximately 0.8 of a chord above the boundary-layer wake may be due to an extended shock or to the effect of the tip vortex on the distribution of the separation losses.

Boundary-layer flow.- The wake measurements indicate that when the Mach number is increased from 0.84 to 0.89 at an angle of attack of 2°, the major portion of the drag coefficient rise for the wing is caused by separation.

The tuft patterns (fig. 10), wake measurements (fig. 14), and pressure recoveries (fig. 4), indicate that, when the Mach number is increased from 0.85 to 0.89, the region of severe separation on the upper surface of the wing with 30° of sweepback at an angle of 2° spreads outward, primarily. The tuft patterns indicate that, at a Mach number of 0.89, severe separation apparently occurs on this surface to approximately the 85-percent-semispan station. The relatively large increase in the severity of separation on the sections outboard of the midsemispan station is believed to be due primarily to a thickening and destabilization of the boundary layer on the outboard region, caused by the outward flow of the low-energy air associated with the separation of the boundary layer on the midsemispan sections.

The tuft patterns and wake measurements indicate that when the Mach number is increased to 0.89, no perceptible separation occurs on the upper surface of sections near the wing-fuselage juncture. The lack of separation near the juncture is also indicated by the severity of the adverse gradient associated with the shock, compared with that on sections farther outboard (fig. 4(d)). The elimination of the separation at the juncture, even though the shock is as strong above this region as it is farther outboard, may be attributed to an effective control of the boundary layer in this region associated with the lateral variations of the spanwise pressure gradients.

The tuft patterns also indicate that the separation of the upper surface of sections inboard of the midsemispan station is considerably less severe than that on sections outboard of that station. This reduction is believed to be associated with the spanwise variation of the energy losses. Because of this variation, the spanwise flow of the boundary layer shown by the tufts (fig. 10(e)) removes more low-energy

air from a given area in this region toward the outboard sections than it induces into this area from the inboard region, where the relative level of losses is lower. As a result, the boundary layer in this region is thinned and stabilized. Because of the slight spanwise flow of the boundary layer on the inboard sections, indicated by the tuft patterns (fig. 10), the energy deficiency measured behind a given inboard section is somewhat less than that associated with losses in the boundary layer on the section.

The presence of little separation at the tip at a Mach number of 0.89 is indicated by the tuft patterns (fig. 10(e)). The presence of a strong adverse pressure gradient associated with the shock and good pressure recoveries near the trailing edge also indicates the same fact. A similar reduction of separation was observed on the unswept wing at comparable conditions (fig. 7(c) of reference 1). As for the unswept wing, this reduction of separation cannot be attributed completely to a reduction in the strength of the shock. It may be due partly to the sweeping action of the tip vortex.

The tuft patterns (fig. 10(f)) indicate that no separation occurs on the sections near the juncture at a Mach number of 0.925. Since the shock is near the trailing edge of the upper surface of these sections for Mach numbers greater than 0.925, it might be expected that little separation would occur on these sections when the Mach number is increased beyond that value. This expectation leads to the conjecture that little separation due to shock may occur on the upper surface of moderately sweptback wings near the juncture for low angles of attack at all transonic Mach numbers.

Higher Angles of Attack at a Mach Number of 0.60

Boundary-layer flow.- The tuft patterns (figs. 10 and 11) indicate that when the angles of attack of the wings are increased at a Mach number of 0.60, separation occurs initially near the leading edge of sections somewhat outboard of the midsemispan stations. This separation does not lead to a breakdown of the flow on the aft regions of these sections. This phenomenon is common to airfoils with sharp leading edges.

When the angles of attack are increased beyond those of initial separation, the regions of separated flow near the leading edges spread inward and outward, and the flows on the aft regions of sections somewhat outboard of the locations of initial flow breakdown also separate. At the highest test angles of attack no separation was present on the aft regions of the inboard sections of the wings. These indications of the tufts are generally similar to those obtained from comparable wings at similar Mach number and angle-of-attack conditions in the Langley 16-foot high-speed tunnel (reference 8).

Higher Angles of Attack at High Subsonic Mach Numbers

Pressure distributions.- Generally, when the Mach number is increased to high subsonic values at an angle of attack of 7°, the changes in the pressure distributions on the midsemispan sections of the sweptback wings (figs. 4 and 5) are similar to those that occur on the same region of the comparable unswept wing at comparable conditions (reference 1). When the Mach number is increased to 0.96, however, the pressure distributions on the midsemispan sections of the wing with 45° of sweep change in a considerably different manner than do the distributions on the unswept wing at a Mach number of 0.80; the region of adverse gradients shifts rearward by a much greater amount. This is believed to be due to the spanwise expansion of the root effects.

Two negative pressure peaks develop on the upper surfaces of the sweptback wings near the wing-fuselage junctures at an angle of attack of 7° when the Mach number is increased to the high subsonic values under consideration (figs. 6 and 7). The forward peak is near the leading edge and extends outward to the tip. The rearward peak is near the 70-percent-chord station at the juncture and near the 50-percent-chord station farther outboard (figs. 4(k), 4(l), 5(g), and 5(h)). A tendency toward a similar double peak on the inboard sections of a wing with an NACA 65-210 section and 45° of sweepback at a Mach number of 0.90 is shown in reference 9. The local velocities associated with the two peaks are supersonic by considerable amounts. The peak negative pressures measured near the leading edge of the root sections of the sweptback wings are believed to be considerably greater than they would have been if the fuselage had not been present, as in the case with the comparable unswept wing (reference 1).

Near the tips, the rearward shifts of the adverse pressure gradients are much less pronounced than they are farther inboard, as for lower angles of attack at higher Mach numbers.

Shocks.- The wake measurements made behind the wings with 30° and 45° of sweepback at Mach numbers of 0.80 and 0.89 for angles of attack of 8° and 6°, respectively, (figs. 12(b) and 13), indicate the presence of strong shocks along almost the entire upper surfaces of the wings at these conditions.

An analysis of the pressure distributions for 7° angle of attack leads to the conjecture that shocks do not form behind the forward negative pressure peaks near the wing-fuselage junctures.

Boundary-layer flow.- When the Mach number is increased from 0.60 to high subsonic values, the profile-drag coefficients for the sweptback wings at moderate normal-force coefficients increase, as would be expected,

and then decrease (fig. 18). These reductions are probably caused by changes in the wing-section characteristics rather than any complex three-dimensional phenomena since a similar change occurred for the comparable wing at a comparable normal-force coefficient and Mach number (fig. 18). A similar change is noted in reference 12.

At all conditions for which tuft patterns are available, little separation is indicated on the upper surfaces of the sweptback wings near the wing-fuselage junctures, even though relatively strong shocks are present above these regions for some conditions. This behavior indicates the powerful stabilizing effect of the spanwise pressure gradients.

Fuselage Pressures

Since the fuselage is cylindrical in the region of the wing-fuselage juncture, the pressure coefficients on the fuselage-alone in this region are very nearly zero at the various Mach numbers. Therefore, the variations in the pressures on the fuselage in this region for the complete configurations, as presented in figures 6 and 7, indicate the approximate effect of the wing on the fuselage.

The effect of the wing on the pressure coefficients on the fuselage directly above the juncture at a Mach number of 0.60 for 2° angle of attack is reduced when the wing is sweptback, as would be expected (figs. 6 and 7, and fig. 5 of reference 1). The reduction of this effect is of approximately the same relative magnitude as the reduction of the pressures on the juncture section of the wing. The pressures on the fuselage just behind the trailing edge of the wing-root juncture are considerably more negative when the wing is swept back than when it is unswept. This effect is present on both the upper and lower surfaces.

When the Mach number is increased to high subsonic values, the pressure coefficients on the fuselage become more positive near the leading edge and more negative near the trailing edge of the juncture, as they do with the unswept wing. The rearward movement is considerably greater for the sweptback wings. The presence of relatively high supersonic Mach numbers on the upper surface of the fuselage near the trailing edge of the juncture at the higher stream Mach numbers indicates that the strong shocks on the upper surface of the wing near the juncture at these conditions spread around the fuselage. The pressure distributions and tuft patterns indicate that, as with the unswept wing, these shocks do not generally lead to separation on the fuselage.

The effects of sweepback on the pressure distributions on the fuselage for an angle of attack of 7° are similar to those for an angle of 2° (figs. 6 and 7).

CONCLUSIONS

A study of the pressure distributions, wake measurements, and tuft patterns for wings with 30° and 45° of sweepback, in conjunction with a fuselage, at high subsonic Mach numbers led to the following conclusions:

1. When the Mach number was increased to high subsonic values at low angles of attack, the locations of the peak negative pressure coefficients on the upper surfaces of sections near the wing-fuselage juncture shifted rearward markedly.

2. Some reduction in the profile-drag coefficient with increasing sweepback at subcritical Mach numbers was indicated.

3. For the wing with 30° of sweepback at low angles of attack, separation associated with onset of shock occurred initially on the midsemispan region of the upper surface. When the Mach number was increased to values considerably above the drag-divergence value, the region of most severe separation spread outward.

4. At Mach numbers up to 0.925, no separation was observed near the wing-fuselage juncture on the upper surface of the sweptback wings at all angles of attack, in spite of the fact that strong shocks were present above this region for some conditions.

5. Generally, the spanwise pressure gradients on the sweptback wings resulted in reductions of boundary-layer separation on the inboard sections and aggravations of separation on the outboard sections.

Langley Aeronautical Laboratory
National Advisory Committee for Aeronautics
Langley Air Force Base, Va.

REFERENCES

1. Whitcomb, Richard T.: An Experimental Study at Moderate and High Subsonic Speeds of the Flow over an Unswept Wing in Conjunction with a Fuselage. NACA RM L50L07, 1950.

2. Whitcomb, Richard T.: An Experimental Study at Moderate and High Subsonic Speeds of the Flow over Wings with 30° and 45° of Sweep-forward in Conjunction with a Fuselage. NACA RM L50K28, 1950.

3. Whitcomb, Richard T.: Investigation of the Characteristics of a High-Aspect-Ratio Wing in the Langley 8-Foot High-Speed Tunnel. NACA RM L6H28a, 1946.

4. Whitcomb, Richard T.: An Investigation of the Effects of Sweep on the Characteristics of a High-Aspect-Ratio Wing in the Langley 8-Foot High-Speed Tunnel. NACA RM L6J01a, 1947.

5. Whitcomb, Richard T.: A Compilation of the Pressures Measured on a Wing and Aileron with Various Amounts of Sweep in the Langley 8-Foot High-Speed Tunnel. NACA RM L8A30a, 1948.

6. Baals, Donald D., and Mourhess, Mary J.: Numerical Evaluation of the Wake-Survey Equations for Subsonic Flow Including the Effect of Energy Addition. NACA ARR L5H27, 1945.

7. Luoma, Arvo A., Bielat, Ralph P., and Whitcomb, Richard T.: High-Speed Wind-Tunnel Investigation of the Lateral-Control Characteristics of Plain Ailerons on a Wing with Various Amounts of Sweep. NACA RM L7I15, 1947.

8. Hieser, Gerald, and Whitcomb, Charles F.: Investigation of the Effects of a Nacelle on the Aerodynamic Characteristics of a Swept Wing and the Effects of Sweep on a Wing Alone. NACA TN 1709, 1948.

9. Johnston, J. Ford, and Danforth, Edward C. B.: Some Pressure-Distribution Measurements on a Swept Wing at Transonic Speeds by the NACA Wing-Flow Method. NACA RM L7D22, 1947.

10. Edwards, George G., and Boltz, Frederick W.: An Analysis of the Forces and Pressure Distribution on a Wing with the Leading Edge Swept Back 37.25°. NACA RM A9K01, 1950.

11. Jones, Robert T.: Subsonic Flow over Thin Oblique Airfoils at Zero Lift. NACA Rep. 902, 1948.

12. Daley, Bernard M., and Lord, Douglas R.: Aerodynamic Characteristics of Several 6-Percent-Thick Airfoils at Angles of Attack from 0° to 20° at High Subsonic Speeds. NACA RM L9E19, 1949.

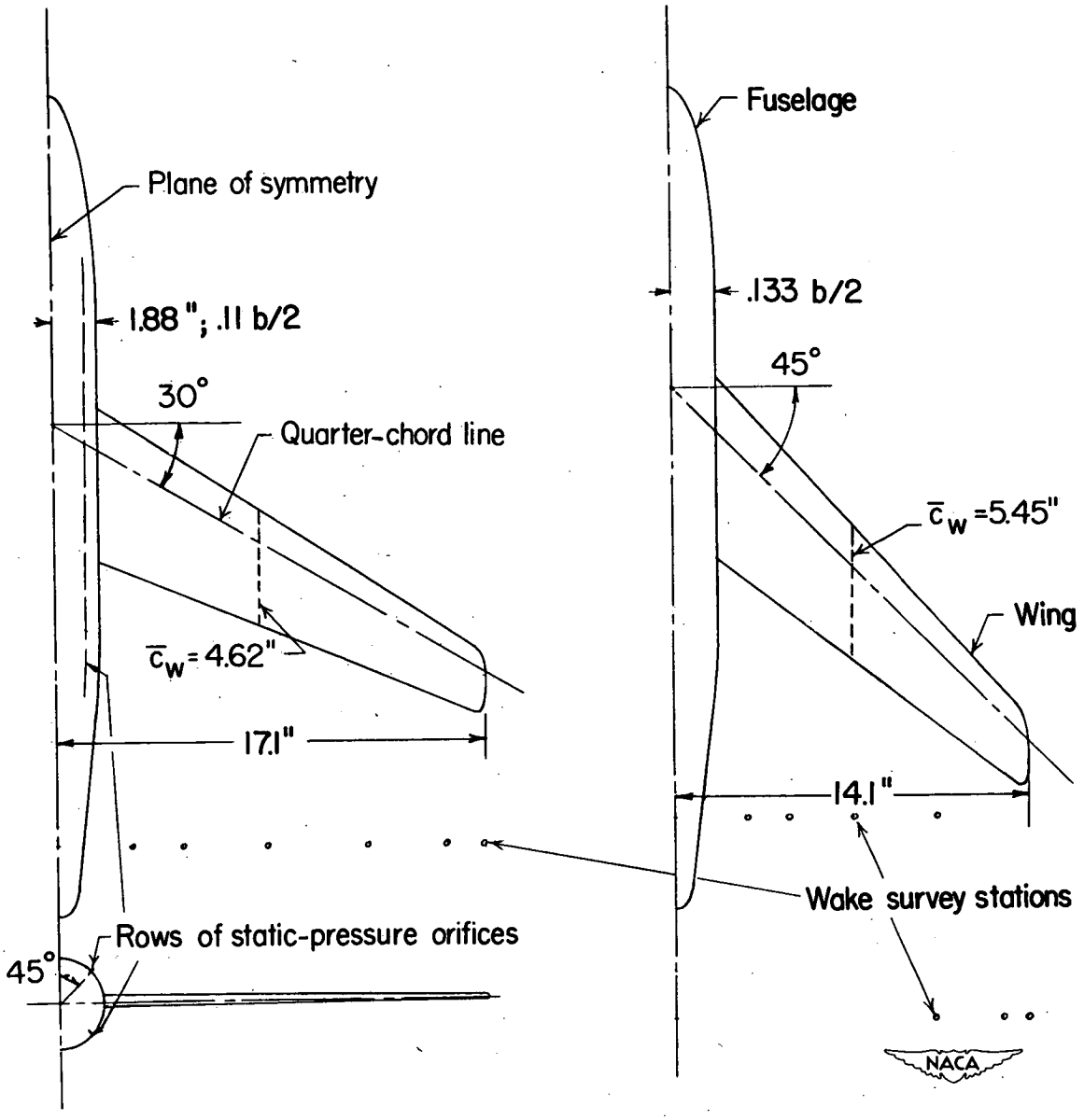

Figure 1.- Configurations.

Page intentionally left blank

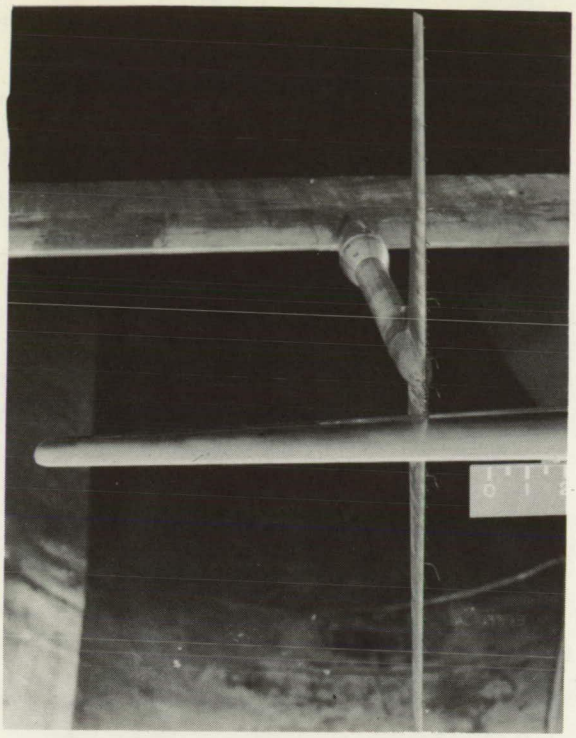

Figure 2.- Wake-survey rake.

L-43593

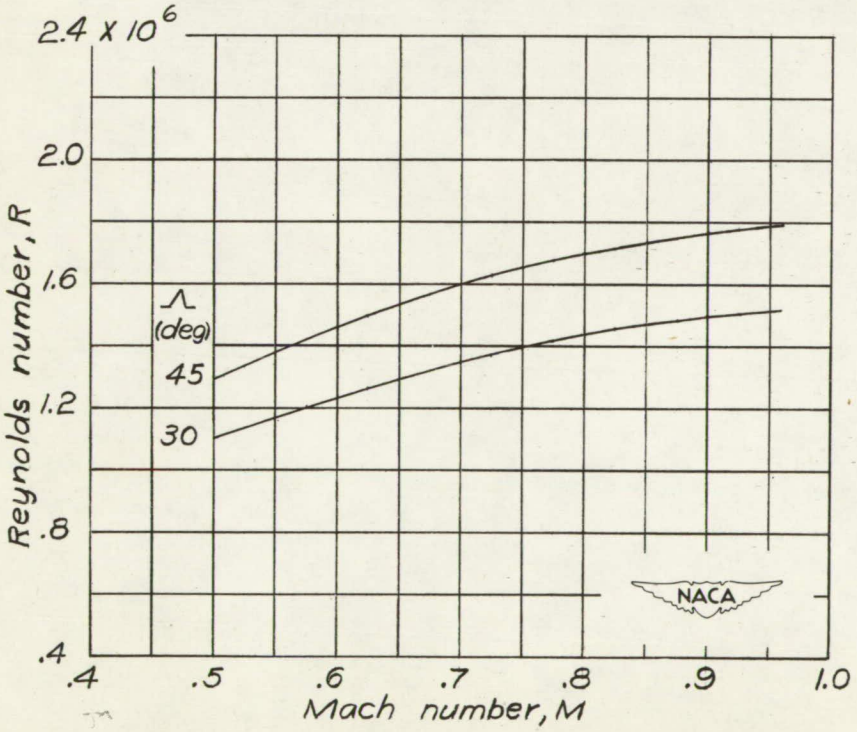

Figure 3.- Variation of Reynolds number with Mach number.

Page intentionally left blank

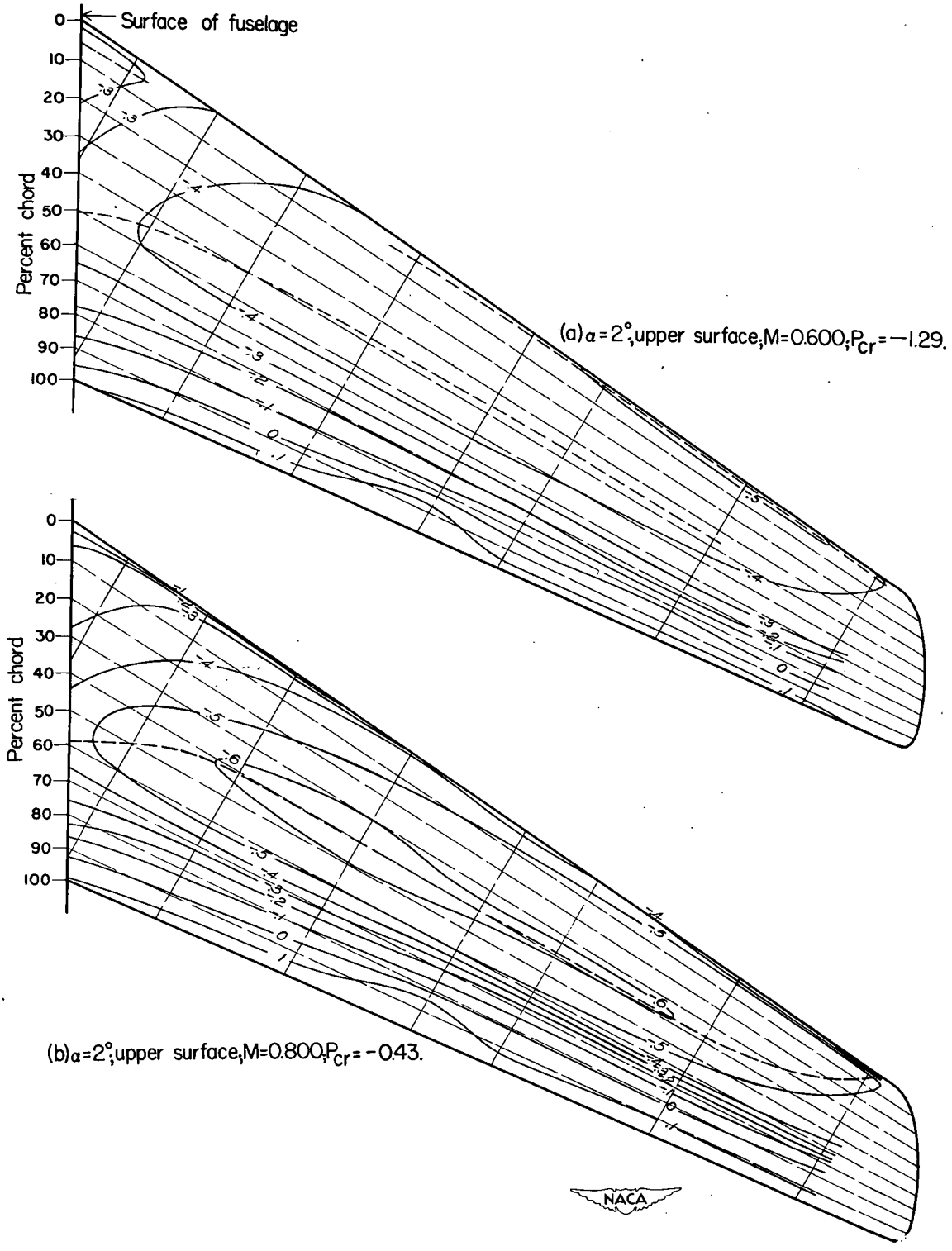

Figure 4.- Equal pressure-coefficient contours. $\Lambda = 30^{\circ}$.

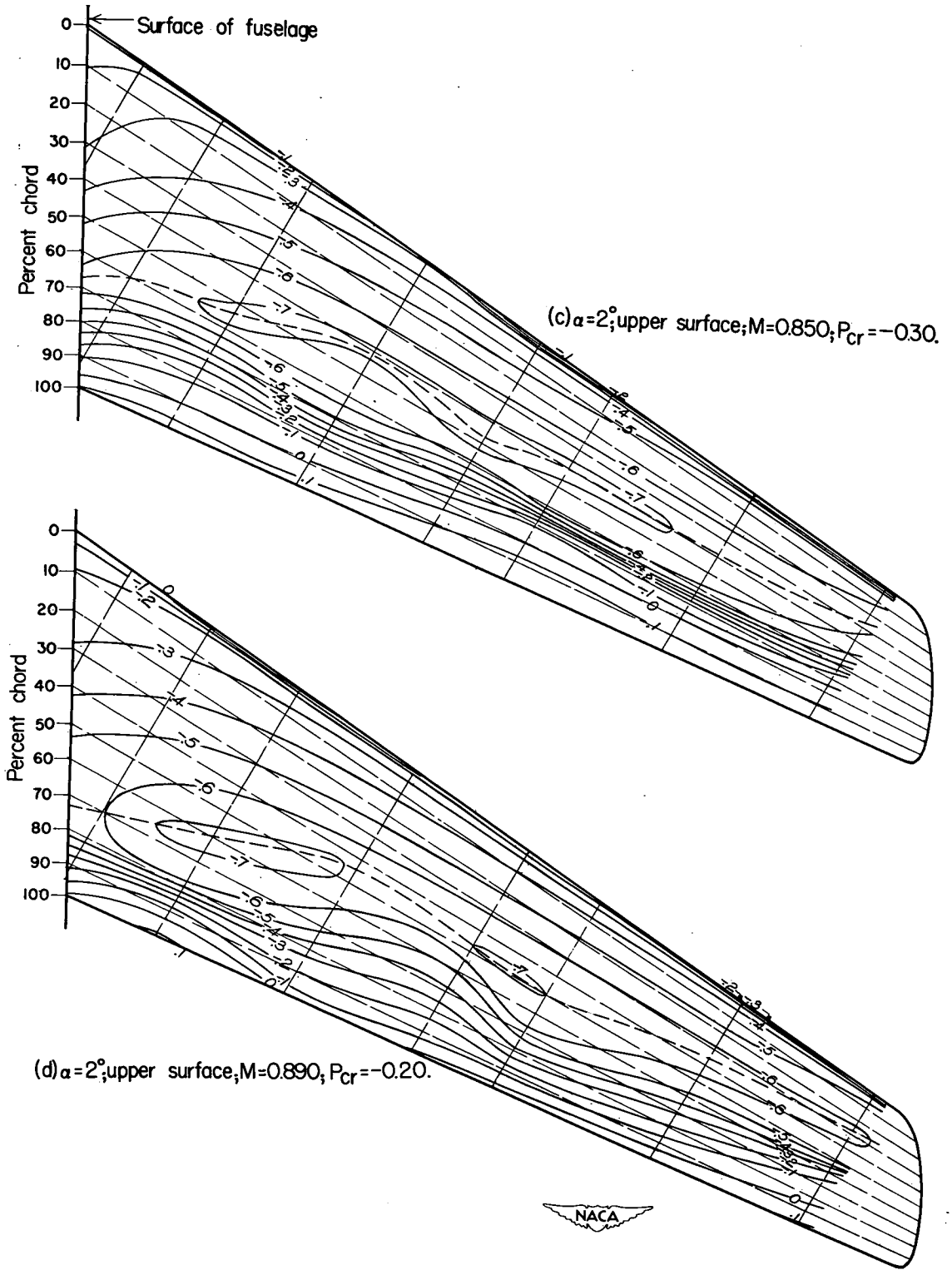

Figure 4.- Continued.

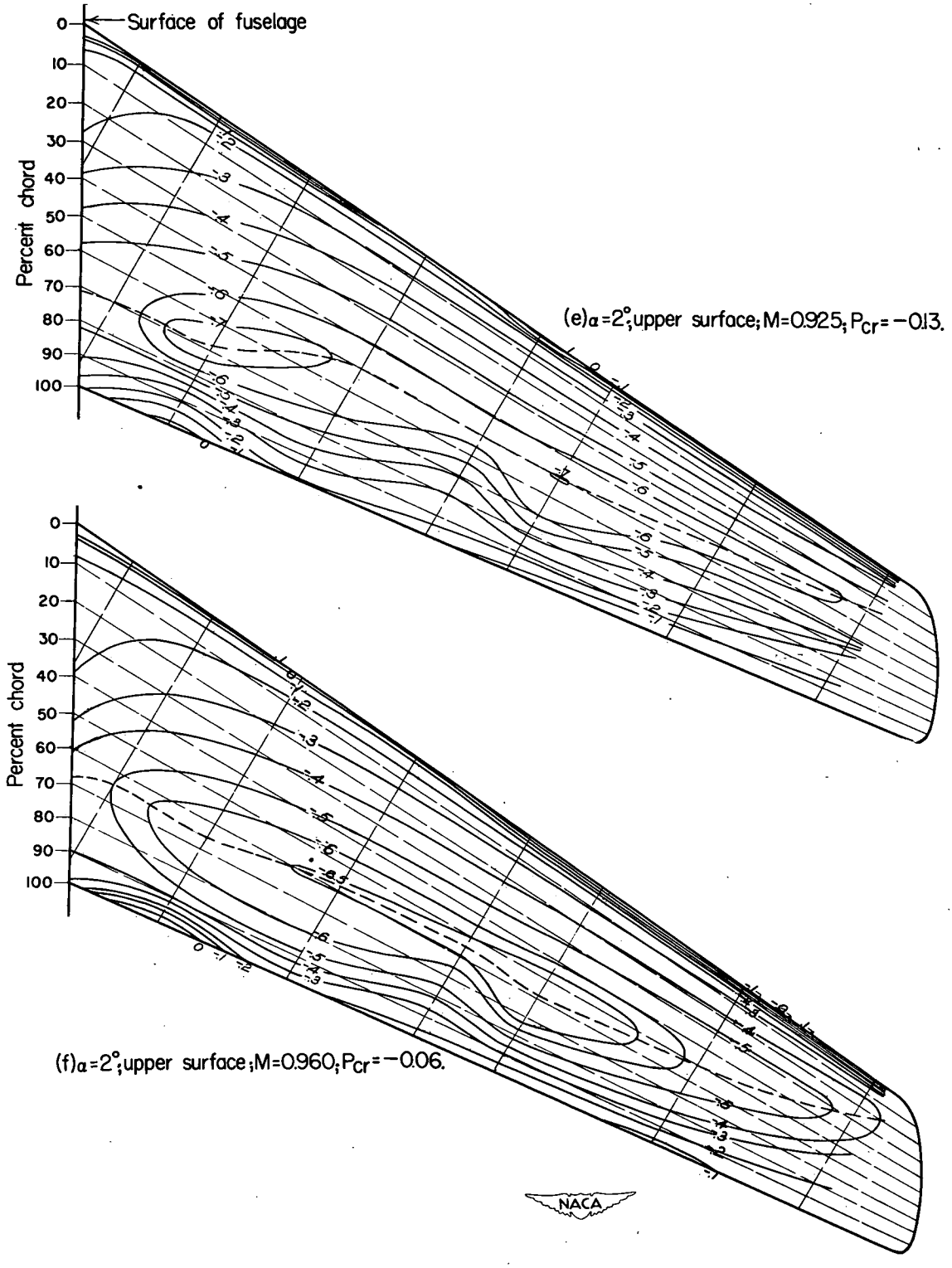

Figure 4.- Continued.

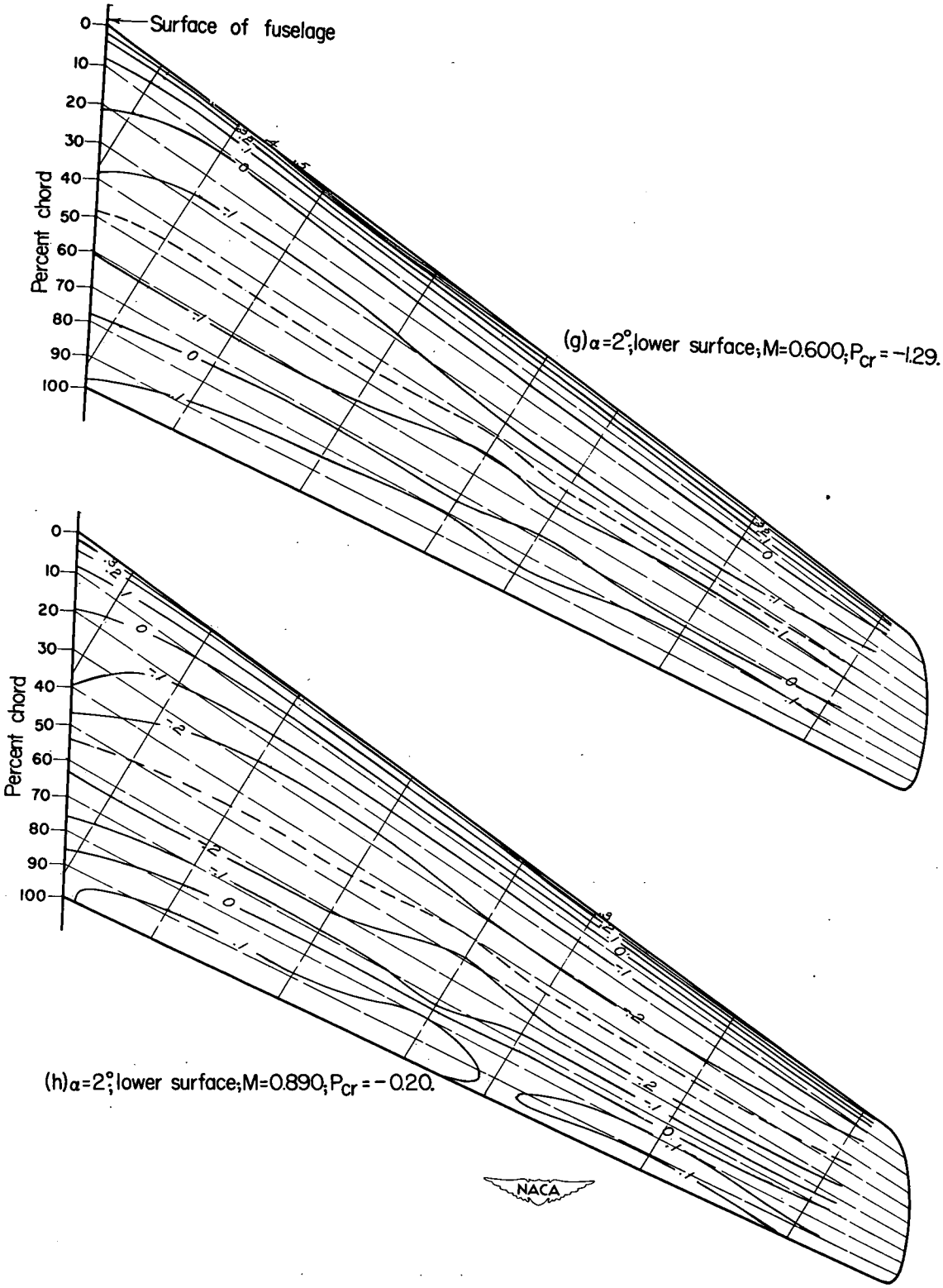

Figure 4.- Continued.

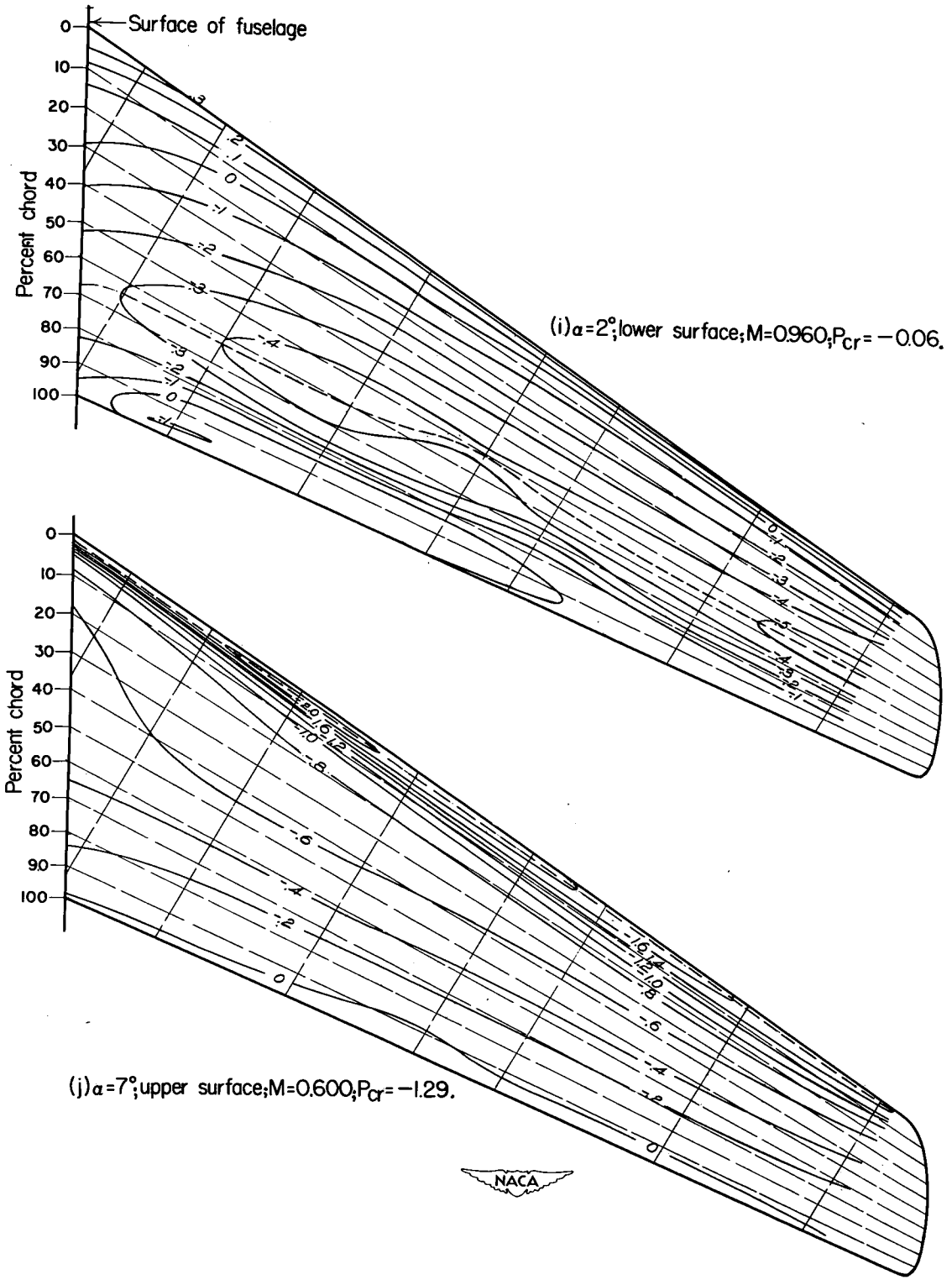

Figure 4.- Continued.

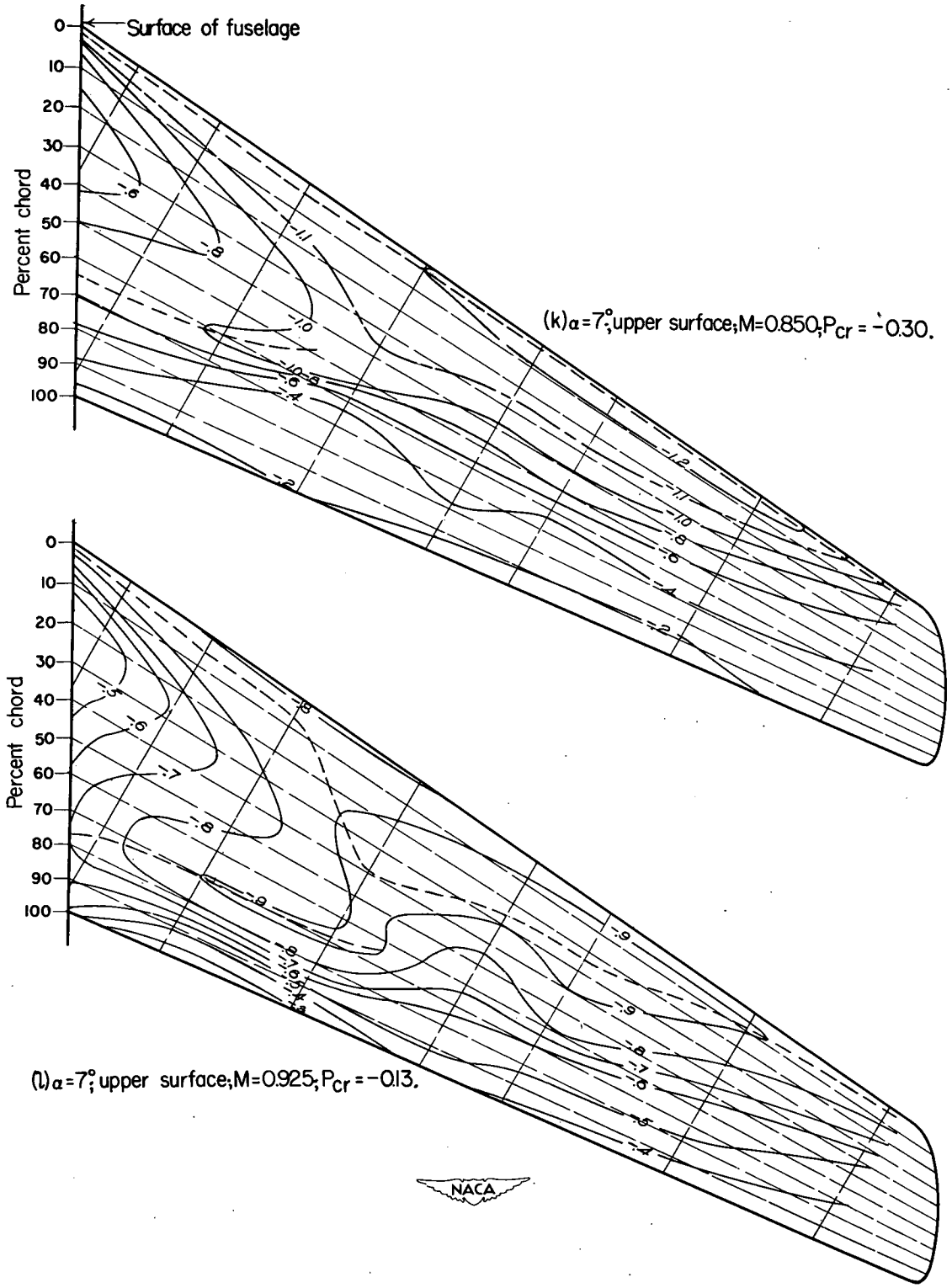

Figure 4.- Continued.

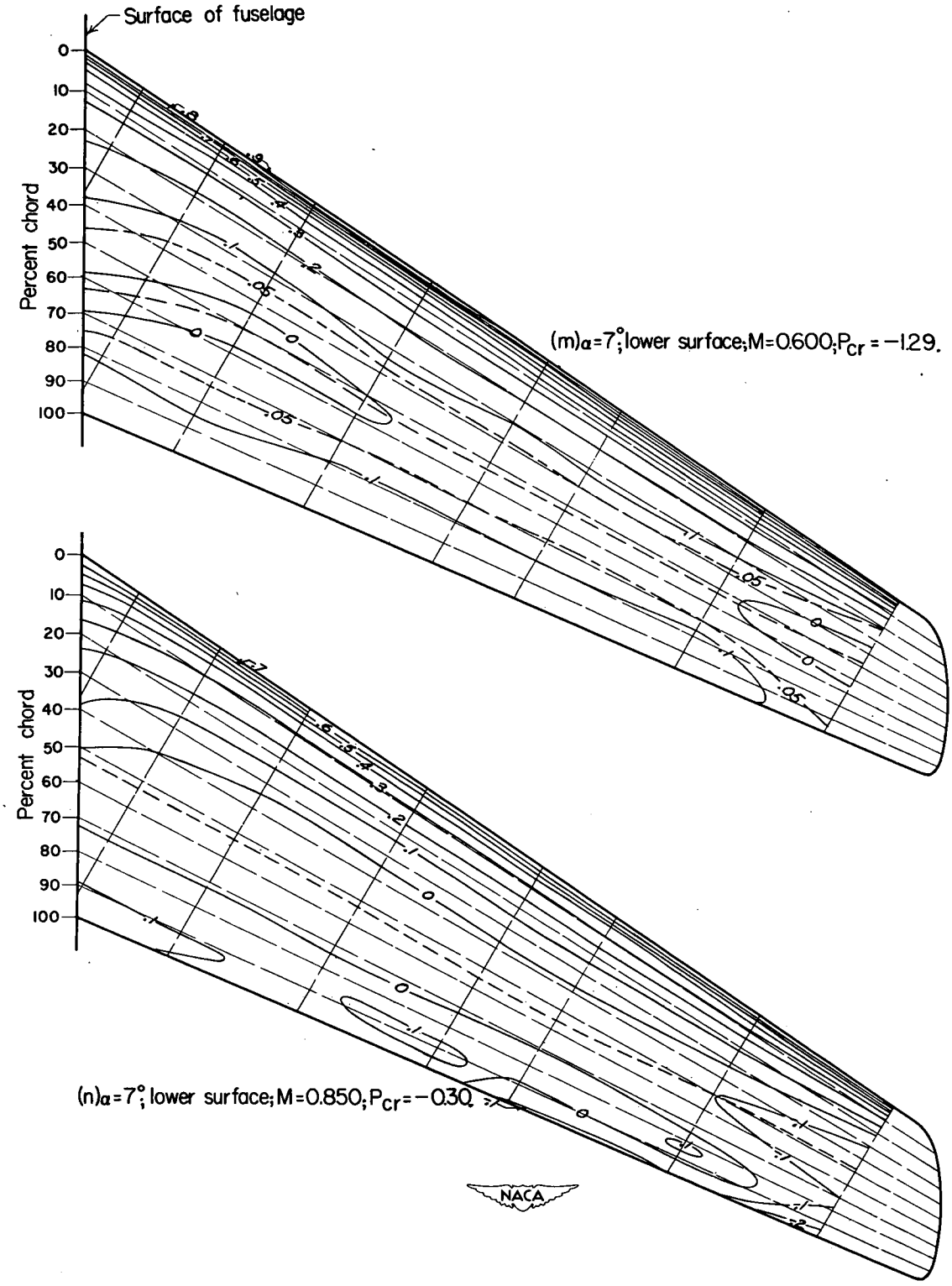

Figure 4.- Concluded.

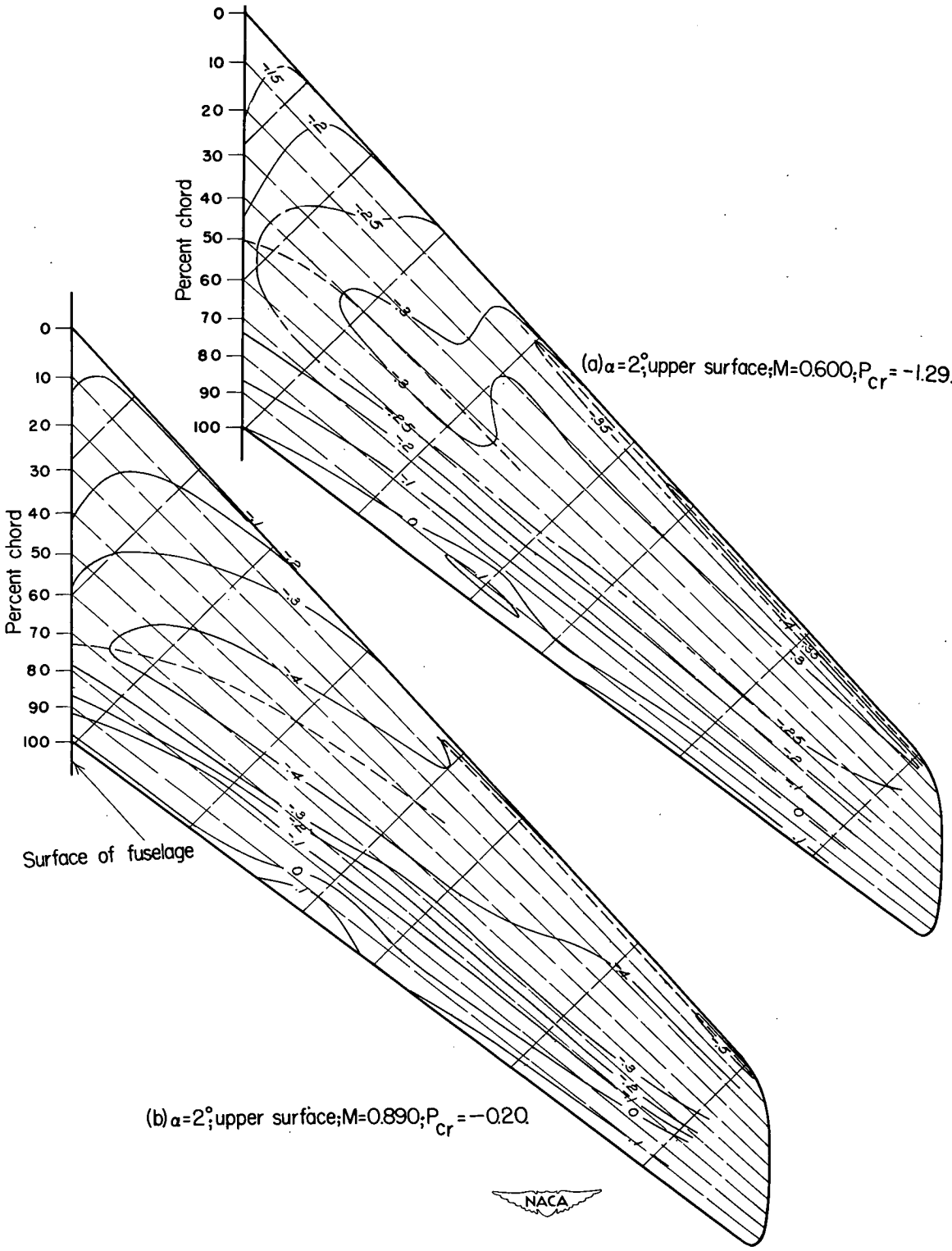

Figure 5.- Equal pressure-coefficient contours. $\Lambda = 45^{\circ}$.

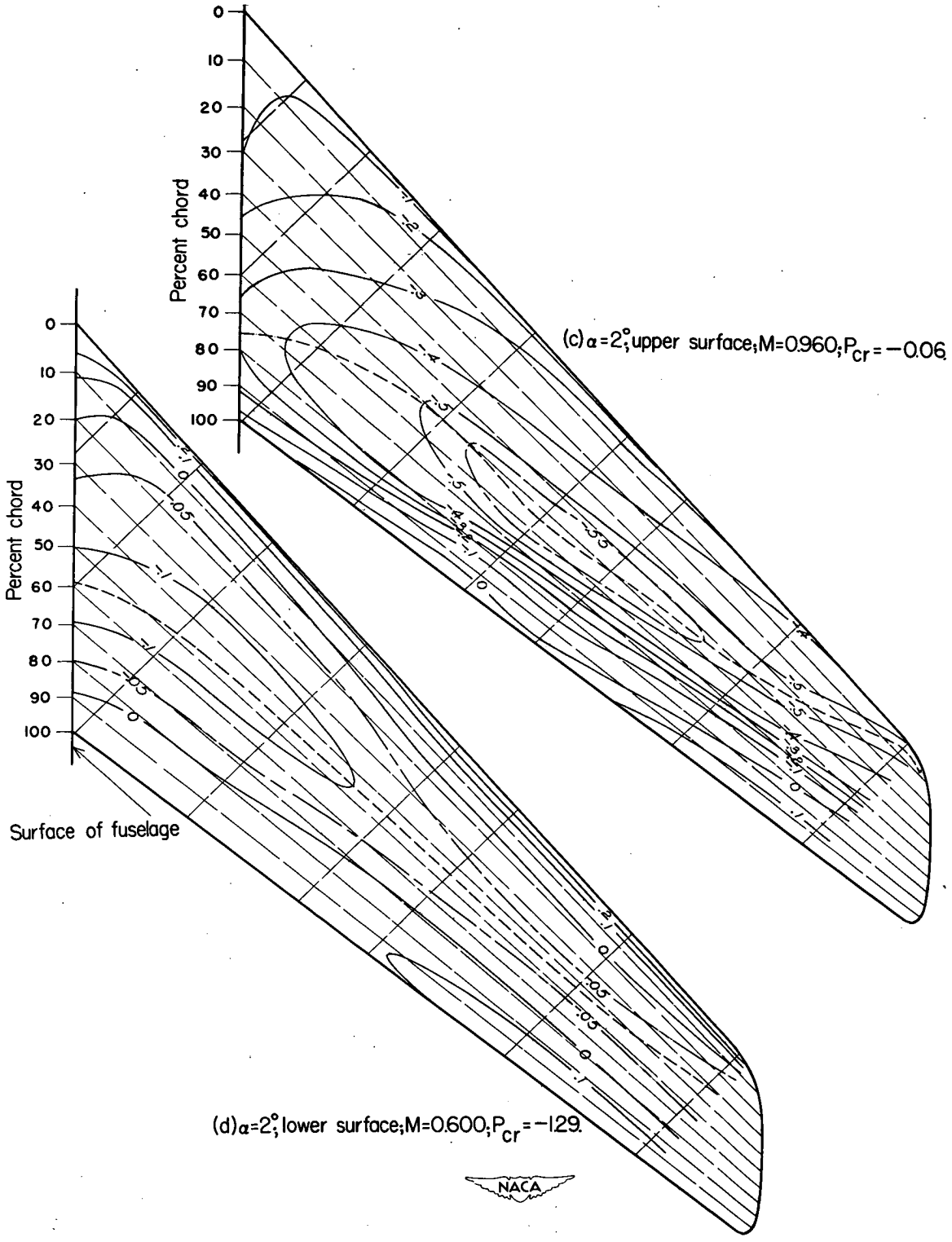

Figure 5.- Continued.

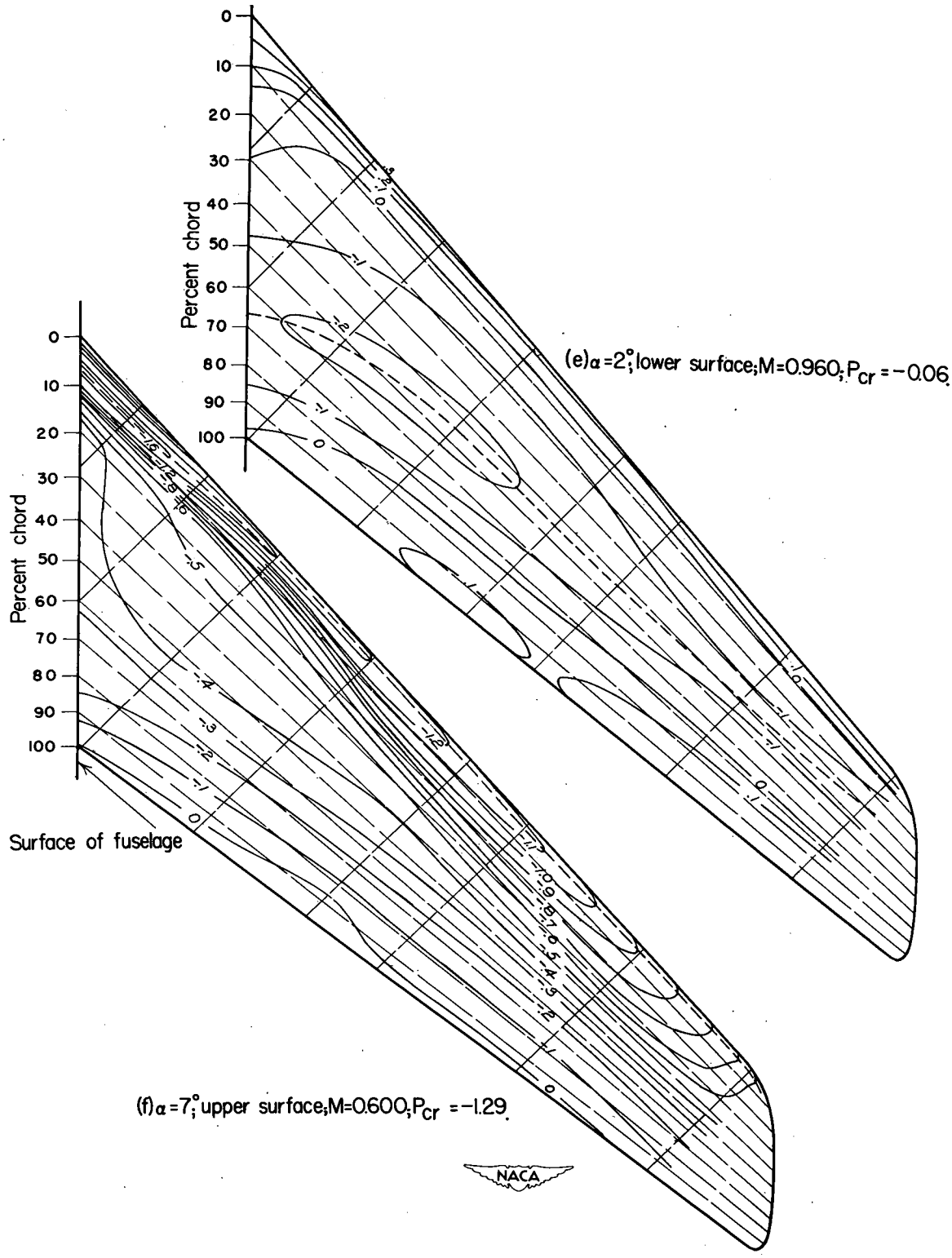

Figure 5.- Continued.

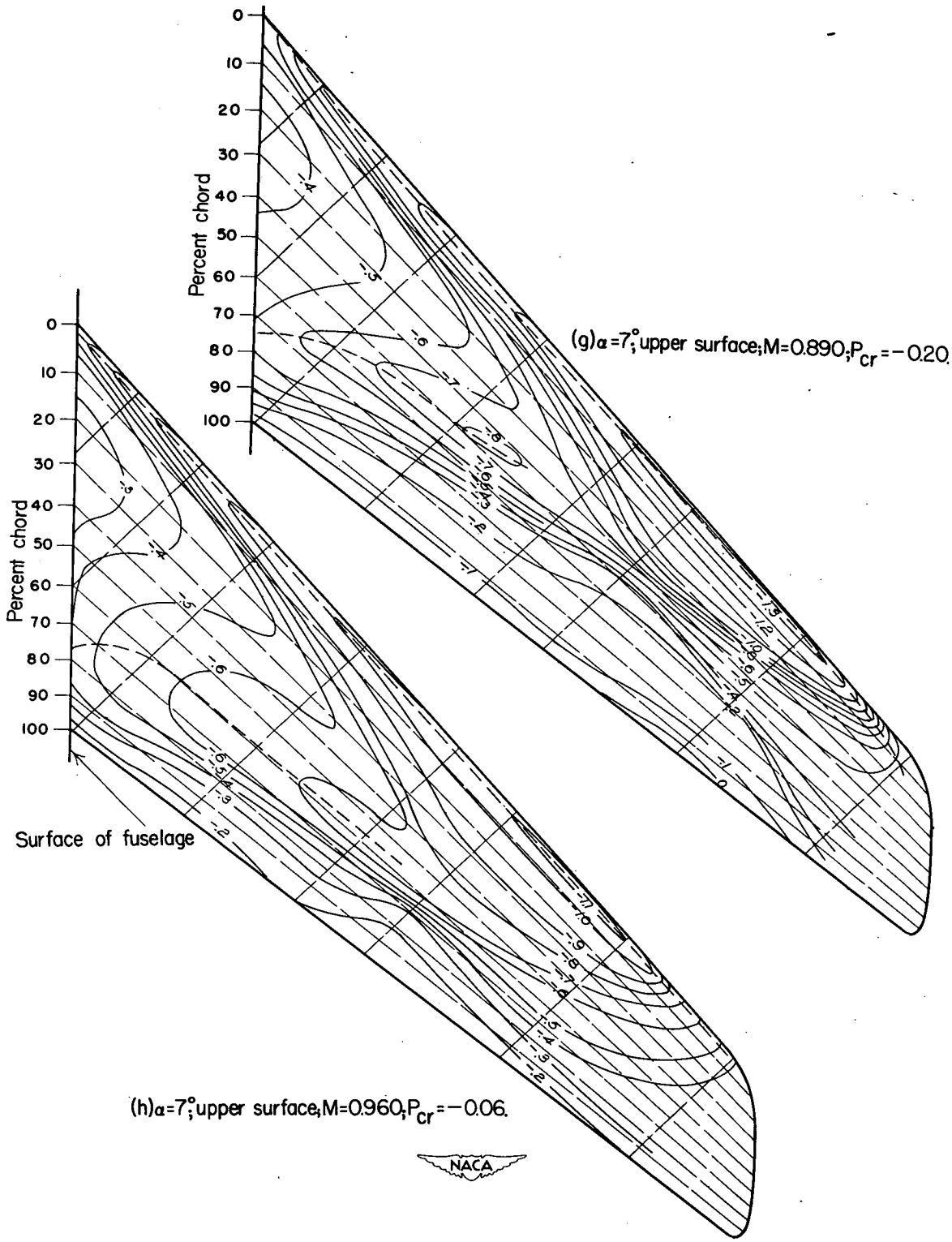

Figure 5.- Continued.

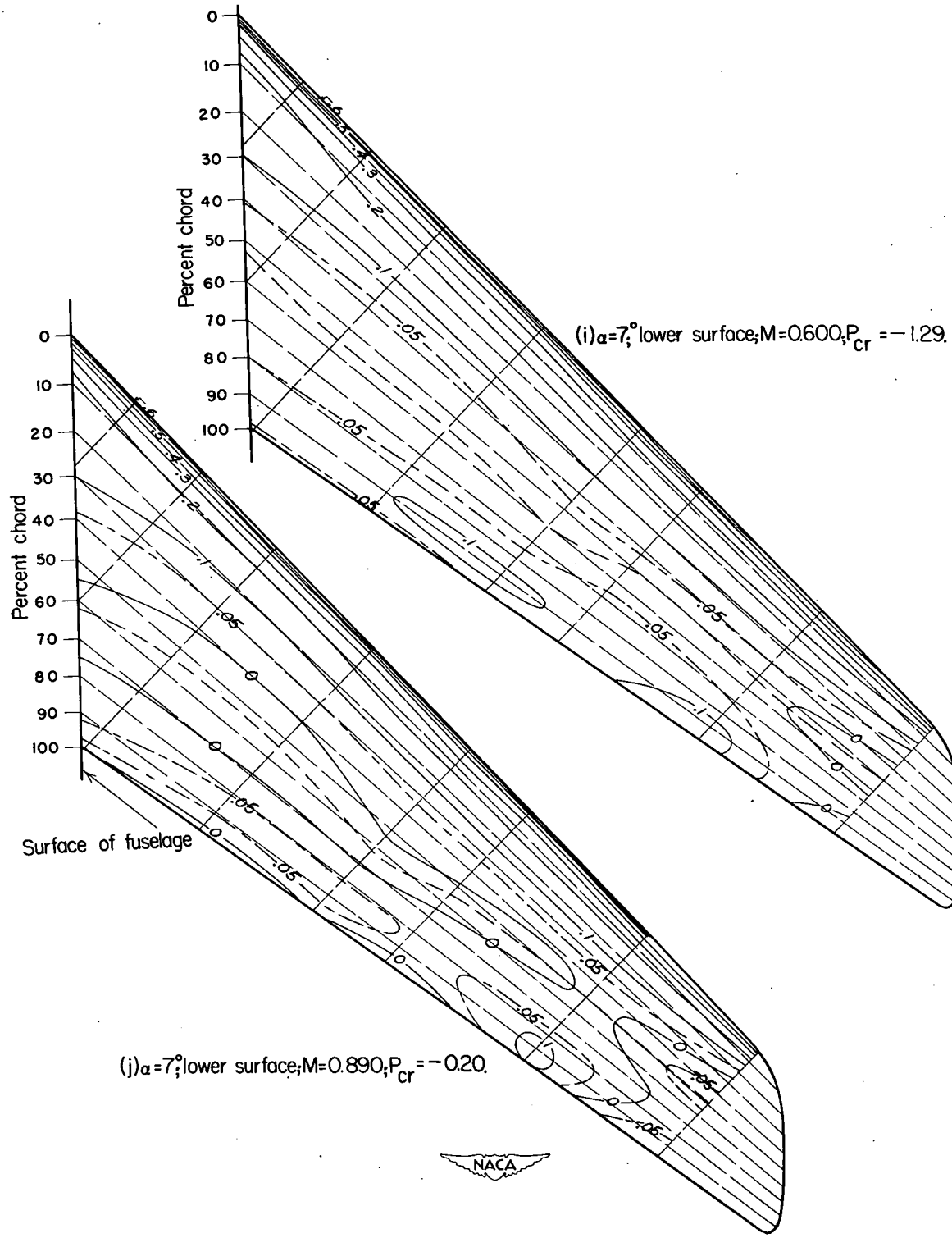

Figure 5.- Concluded.

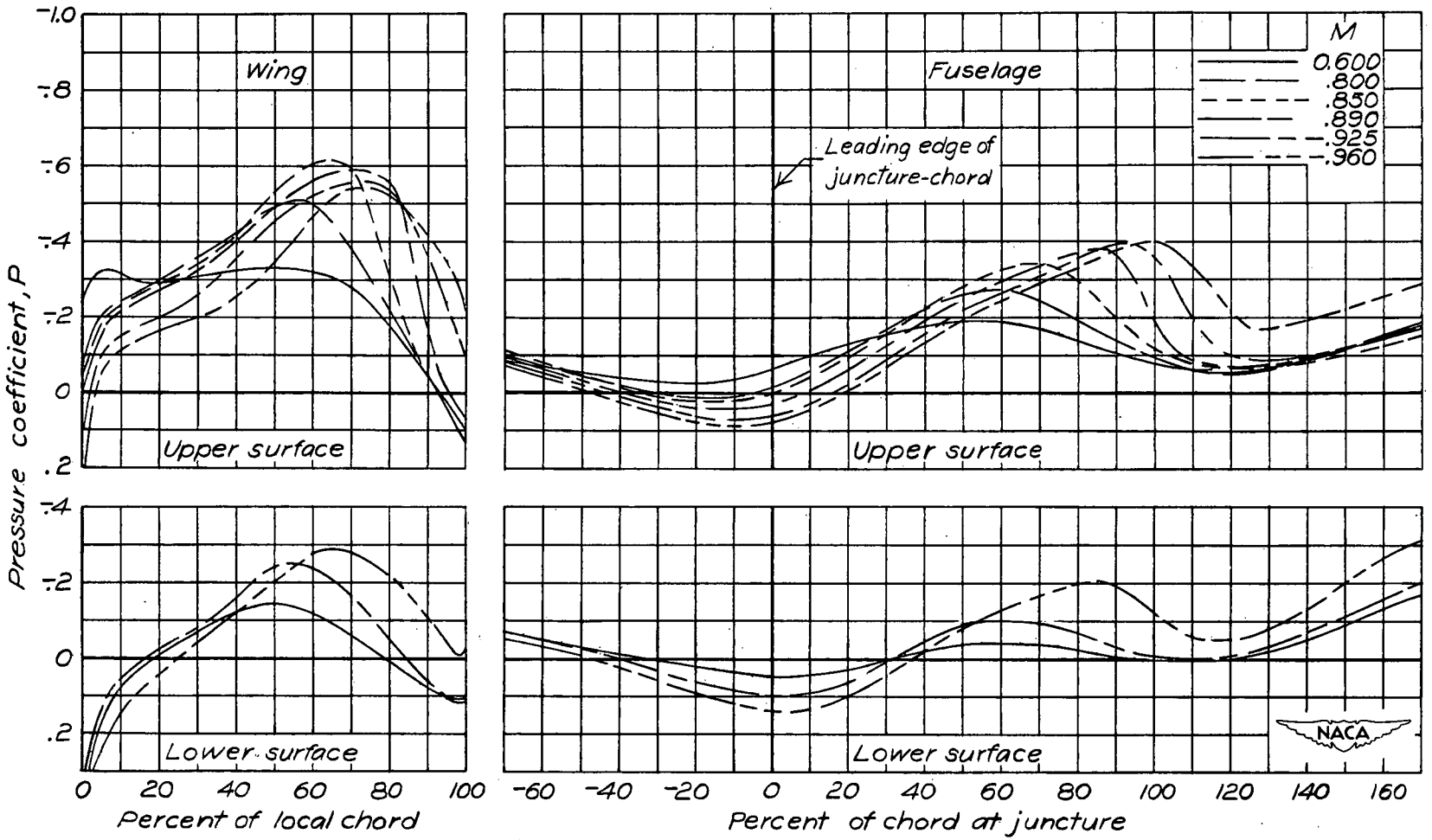

(a) $\alpha = 2^{\circ}$.

Figure 6.- Chordwise pressure distributions near wing-fuselage juncture. $\Lambda = 30^{\circ}$.

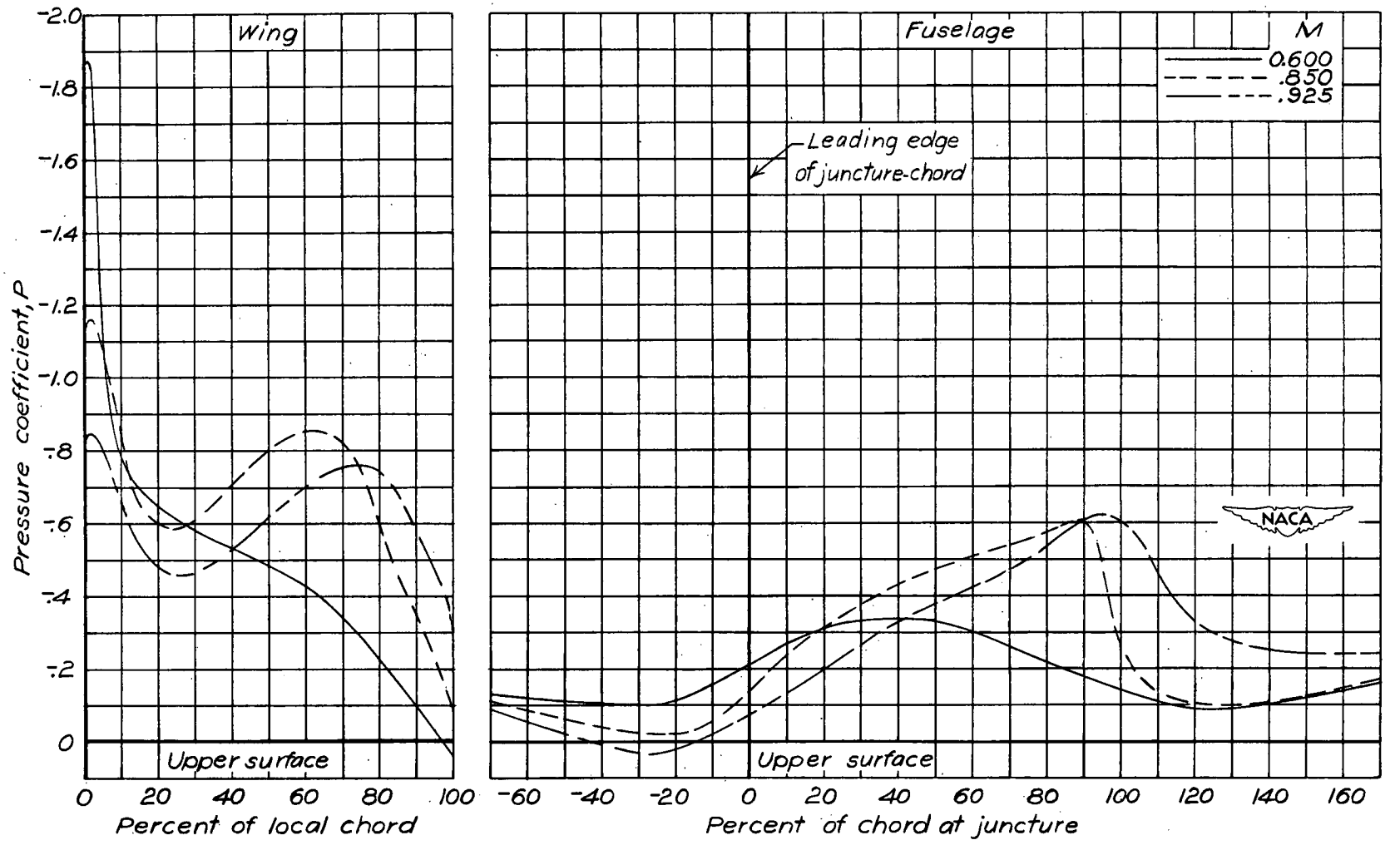

(b) $\alpha = 7^{\circ}$.

Figure 6.- Concluded. $\Lambda = 30^{\circ}$.

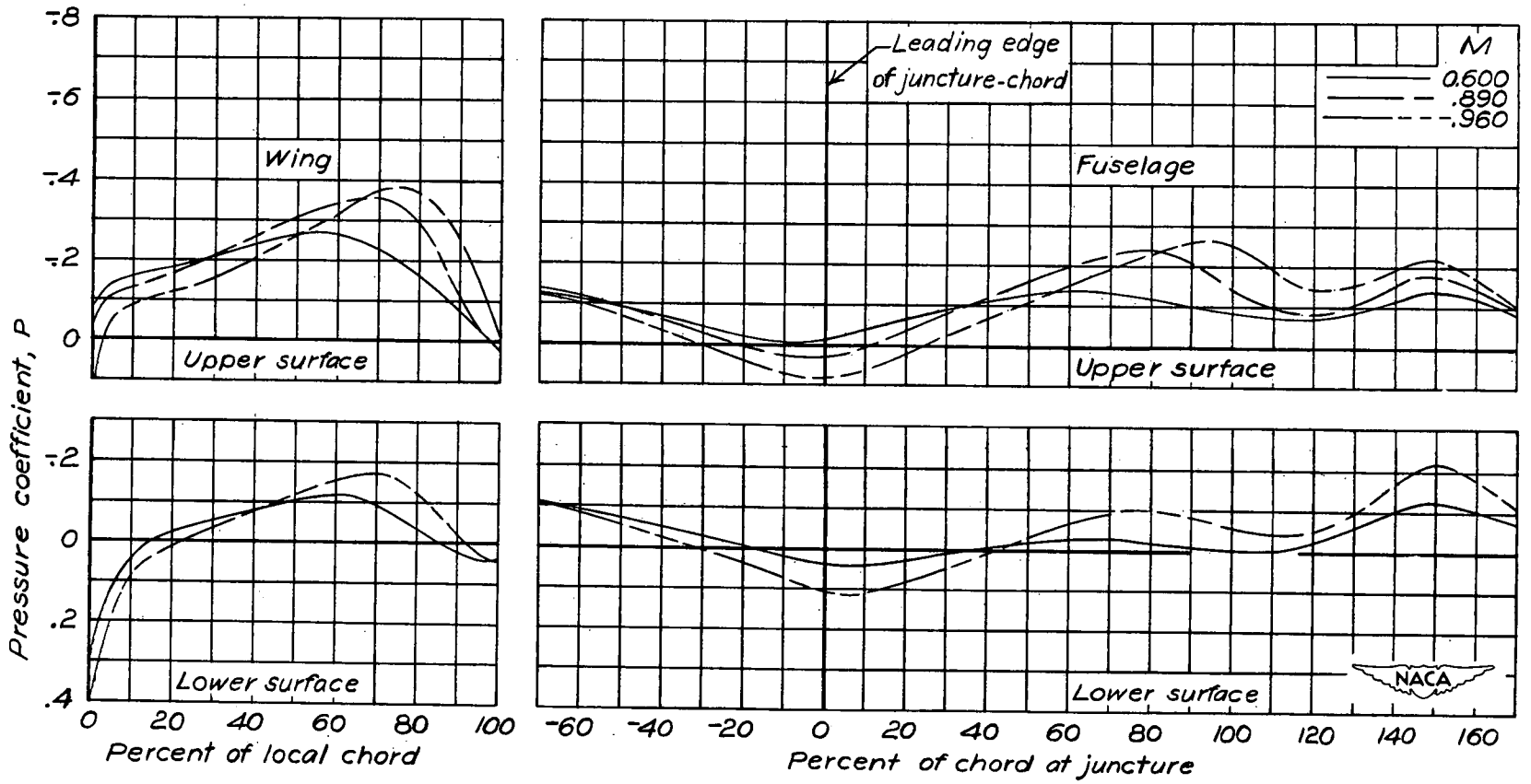

(a) $\alpha = 2^{\circ}$.

Figure 7.- Chordwise pressure distributions near wing-fuselage juncture. $\Lambda = 45^{\circ}$.

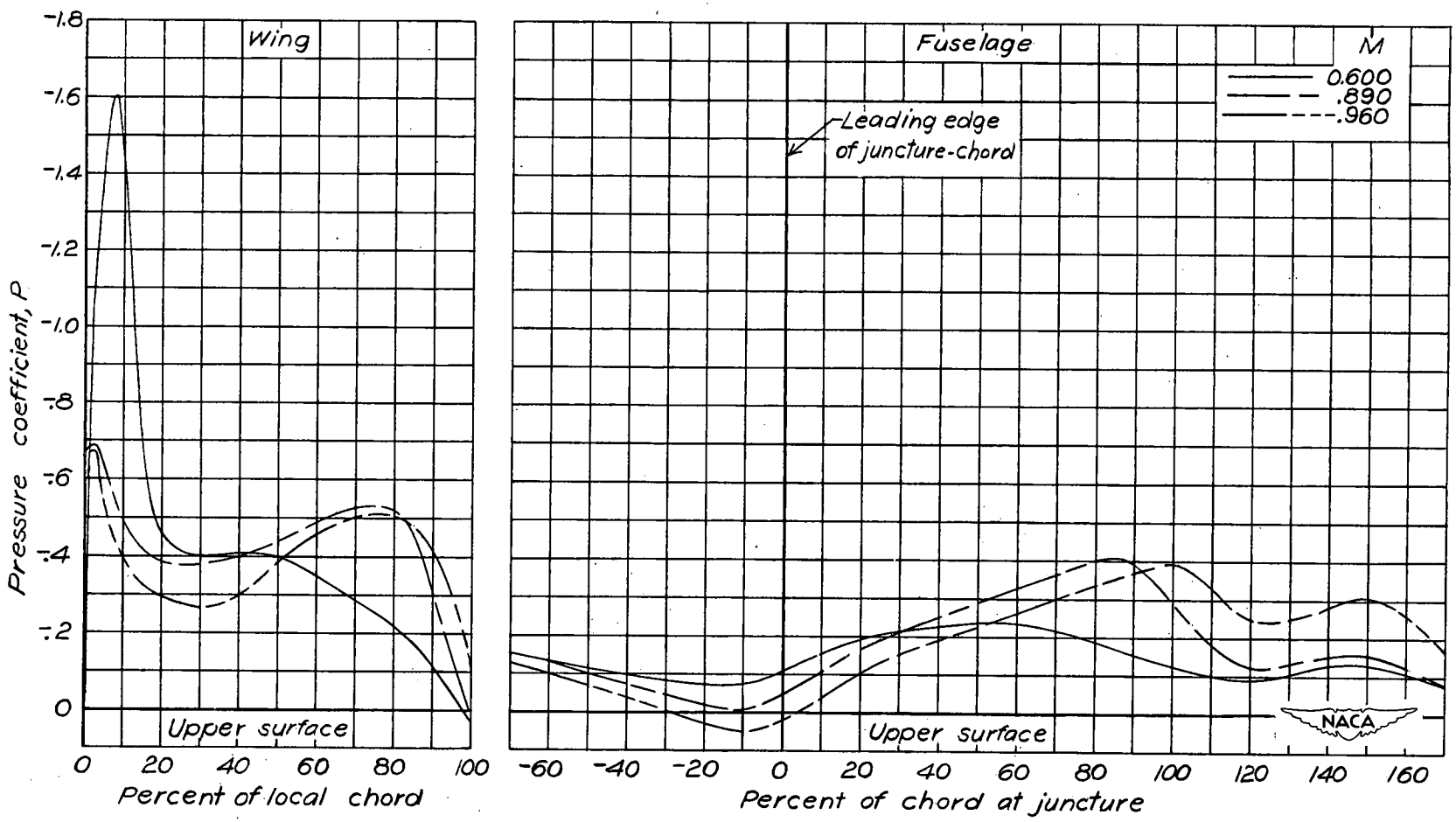

(b) $\alpha = 7^{\circ}$.

Figure 7.- Concluded. $\Lambda = 45^{\circ}$.

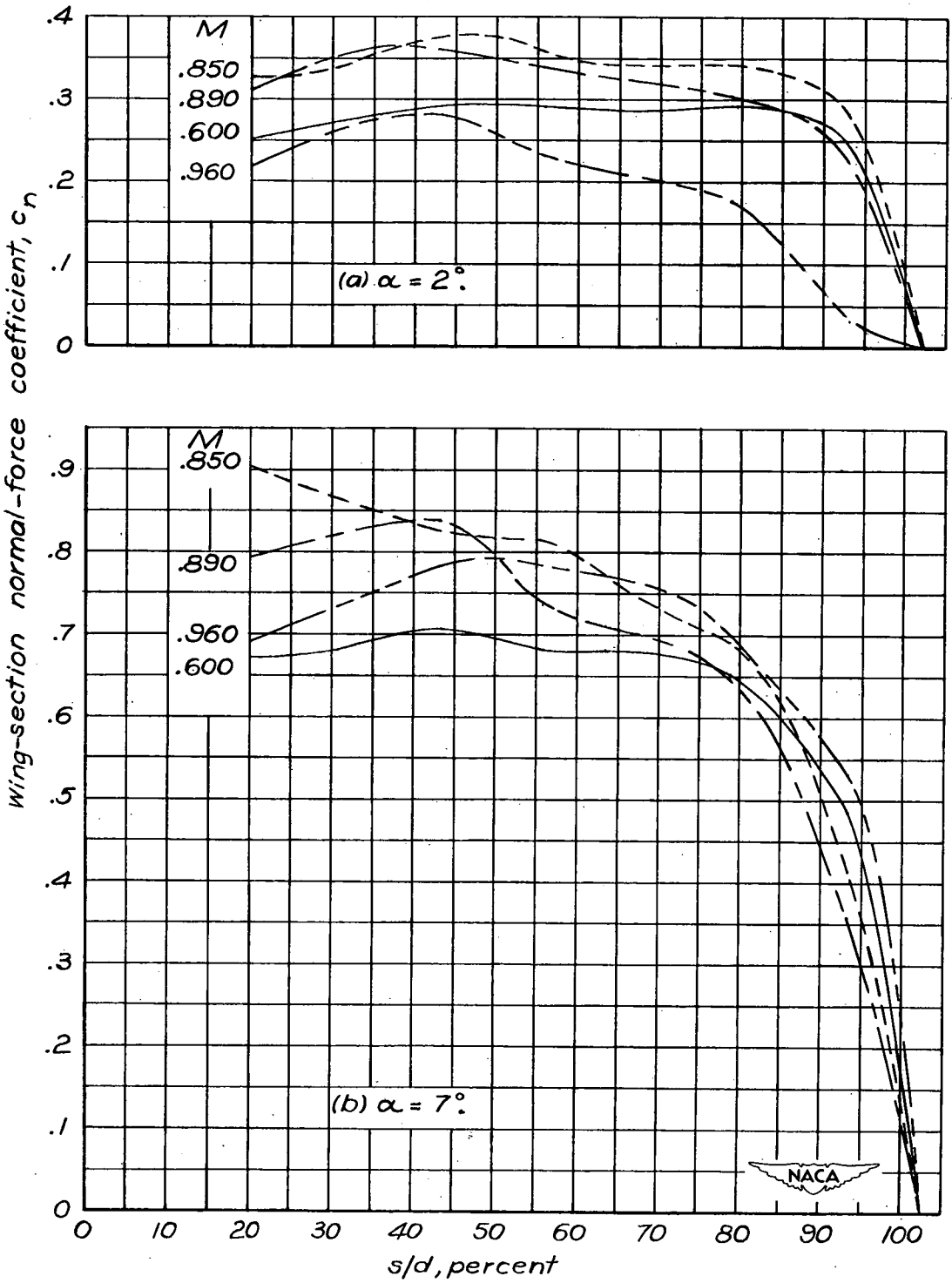

Figure 8.- Spanwise variations of wing-section normal-force coefficient for various Mach numbers. $\Lambda = 30^{\circ}$.

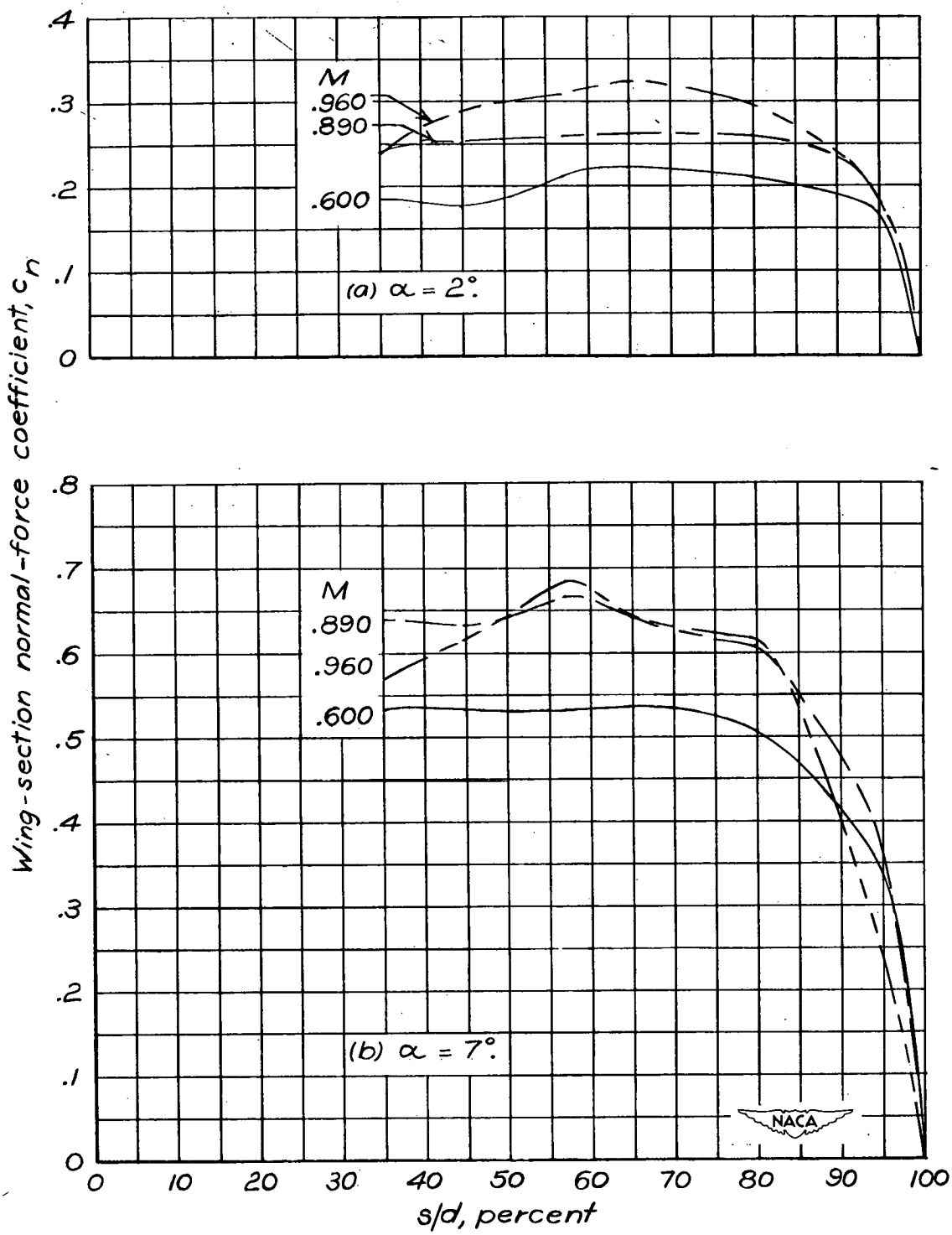

Figure 9.- Spanwise variations of wing-section normal-force coefficient for various Mach numbers. $\Lambda = 45^{\circ}$.

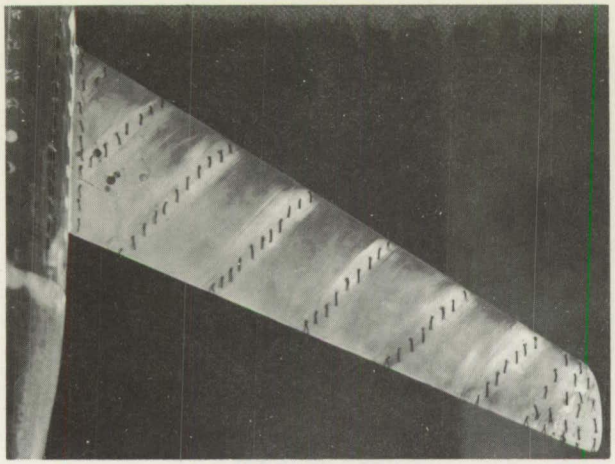

(a) $\alpha = 2^{\circ}$; upper surface; M = 0.60.

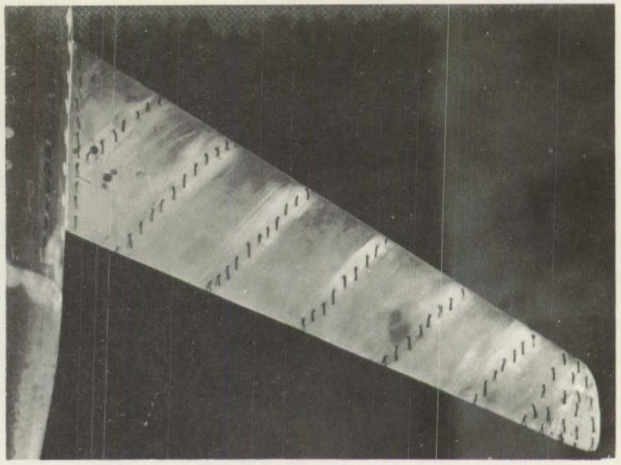

(b) $\alpha = 2^{\circ}$; upper surface; M = 0.75.

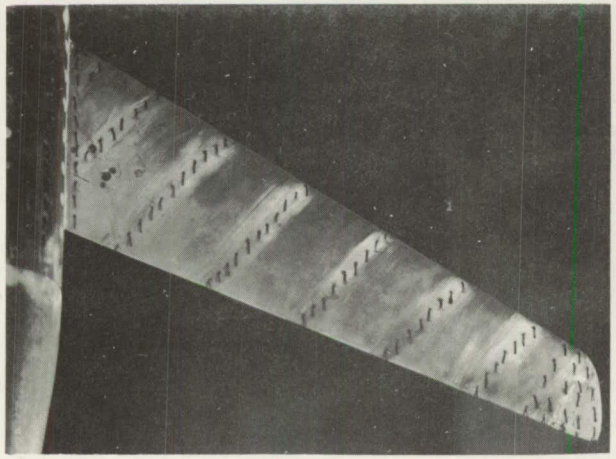

(c) $\alpha = 2^{\circ}$; upper surface; M = 0.80.

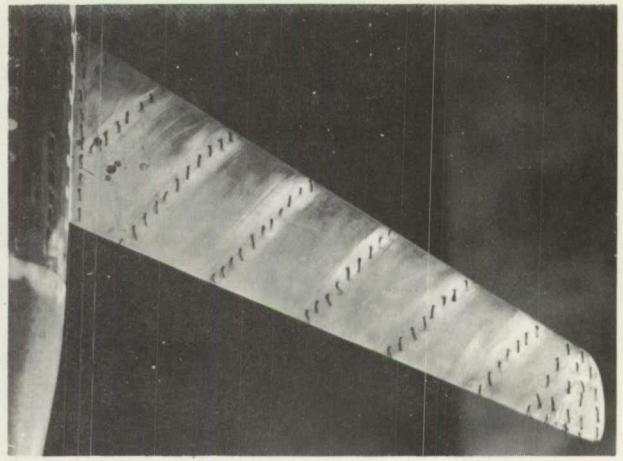

(d) $\alpha = 2^{\circ}$; upper surface; M = 0.85.

NACA

L-68395

Figure 10.- Tuft patterns on wing with 30° of sweepback.

Page intentionally left blank

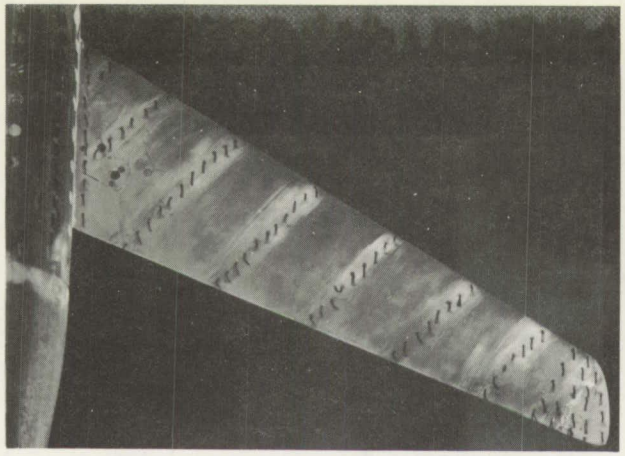

(e) $\alpha = 2^{\circ}$; upper surface; M = 0.89.

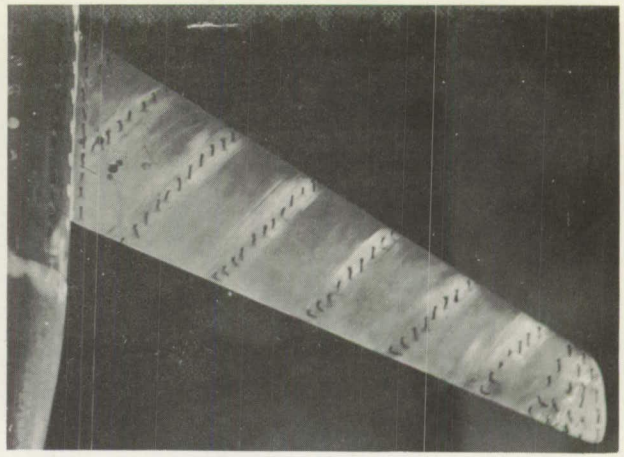

(f) $\alpha = 2^{\circ}$; upper surface; M = 0.925.

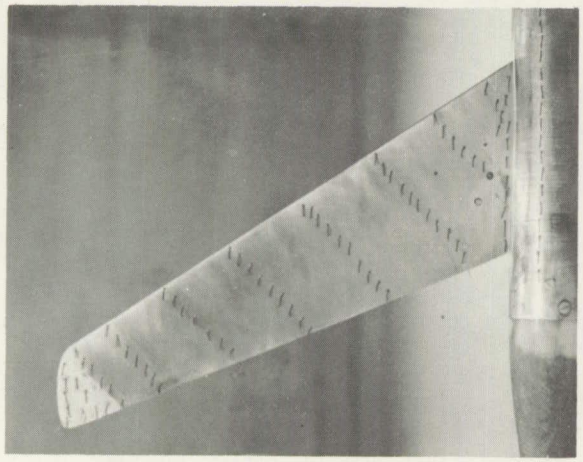

(g) $\alpha = 2^{\circ}$; lower surface; M = 0.60.

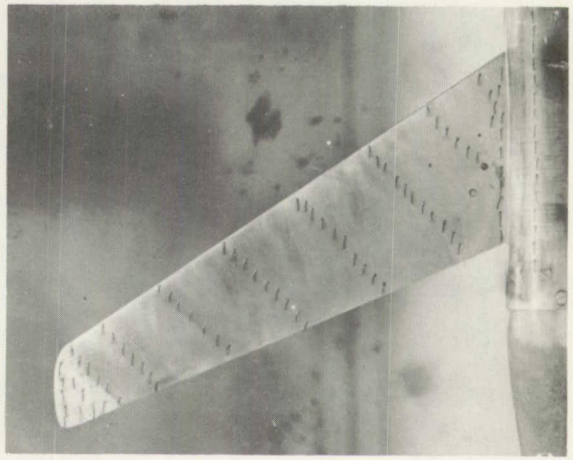

(h) $\alpha = 2^{\circ}$; lower surface; M = 0.925.

NACA

L-68396

Figure 10.- Continued.

Page intentionally left blank

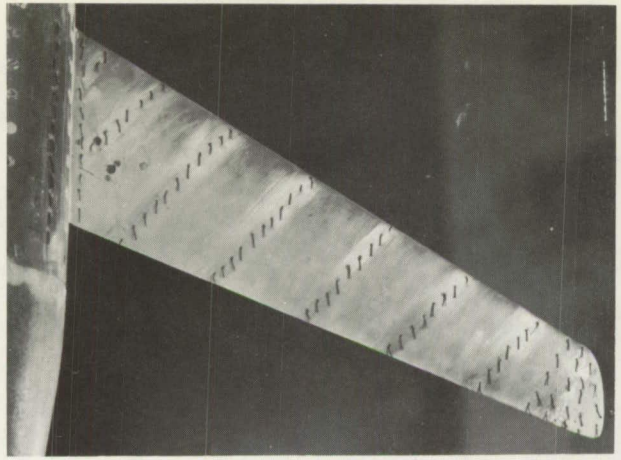

(i) $\alpha = 5^{\circ}$; upper surface; M = 0.60.

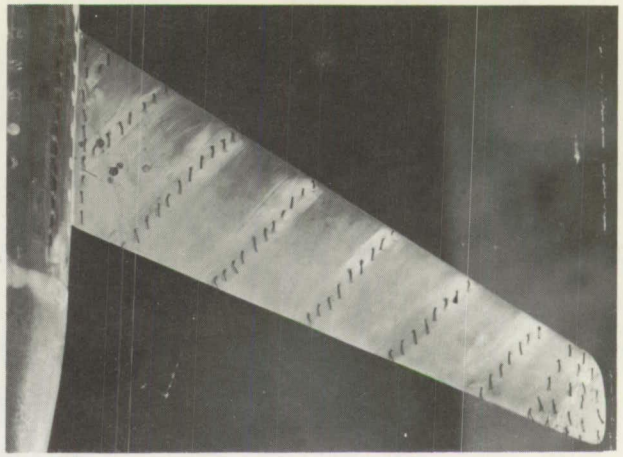

(j) $\alpha = 5^{\circ}$; upper surface; M = 0.80.

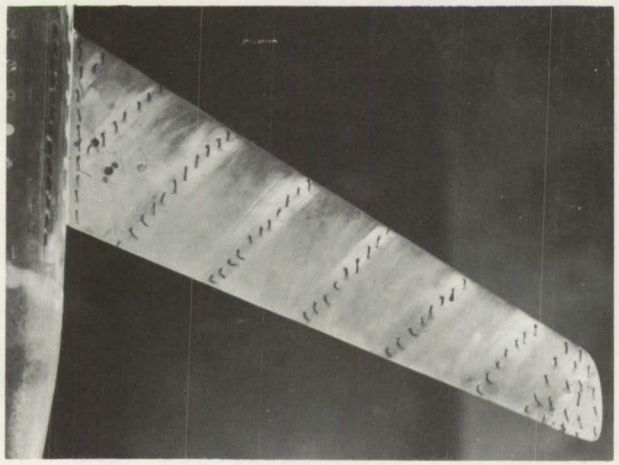

(k) $\alpha = 5^{\circ}$; upper surface; M = 0.85.

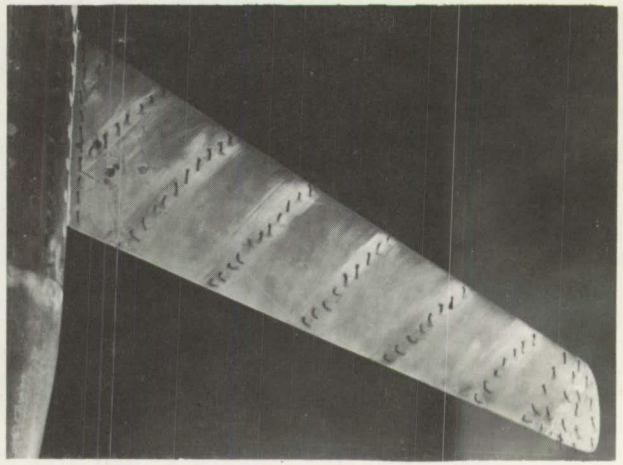

(l) $\alpha = 5^{\circ}$; upper surface; M = 0.89.

NACA

L-68397

Figure 10.- Continued.

Page intentionally left blank

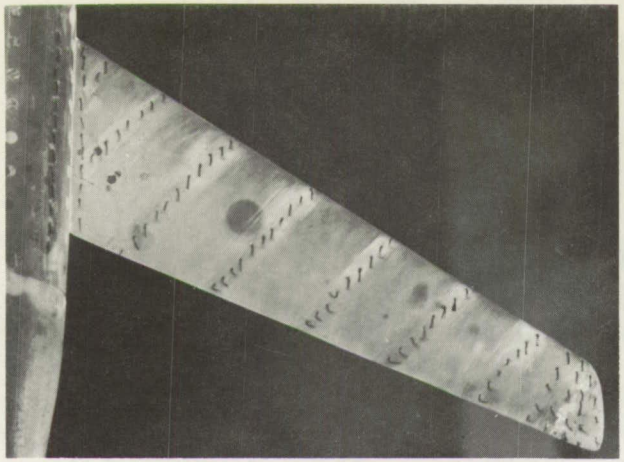

(m) $\alpha = 5^{\circ}$; upper surface; M = 0.925.

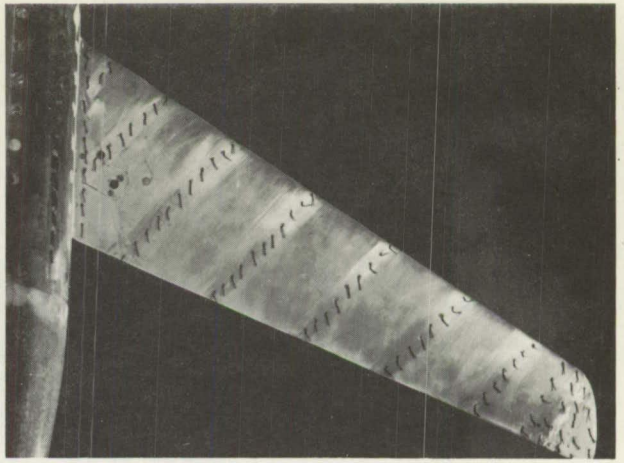

(n) $\alpha = 8^{\circ}$; upper surface; M = 0.60.

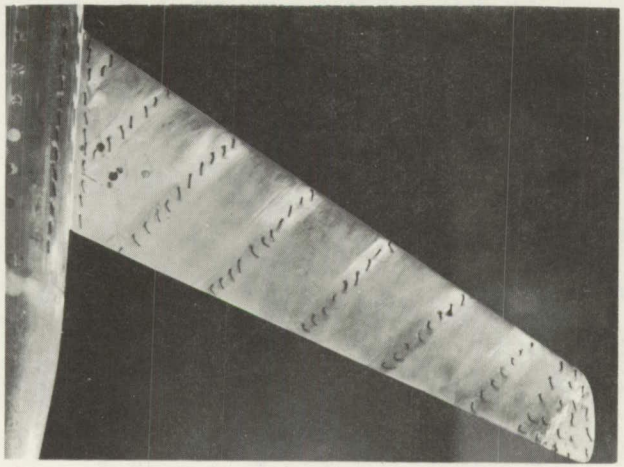

(o) $\alpha = 8^{\circ}$; upper surface; M = 0.80.

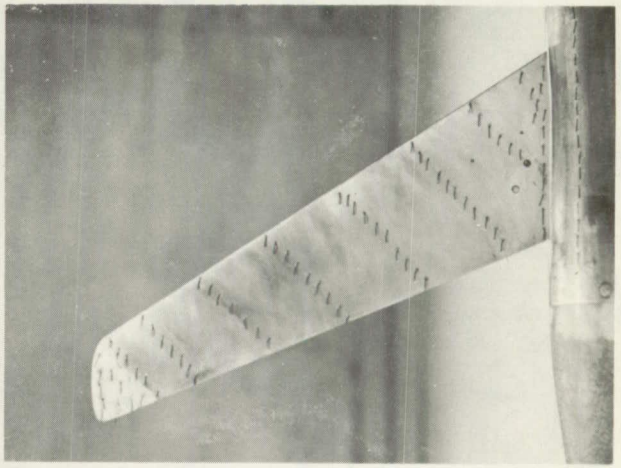

(p) $\alpha = 8^{\circ}$; lower surface; M = 0.60.

NACA

L-68398

Figure 10.- Concluded.

Page intentionally left blank

(a) $\alpha = 3^{\circ}$; upper surface; M = 0.60.

(b) $\alpha = 3^{\circ}$; upper surface; M = 0.925

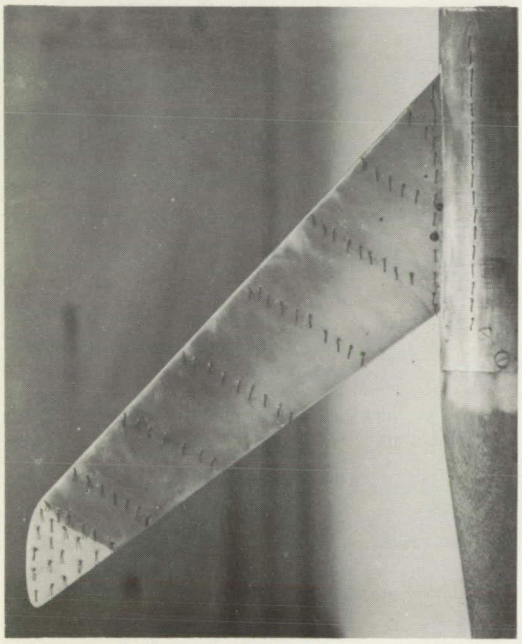

(c) $\alpha = 3^{\circ}$; lower surface; M = 0.60.

(d) $\alpha = 6^{\circ}$; upper surface; M = 0.60.

NACA

L-68399

Figure 11.- Tuft patterns on wing with 45° of sweepback.

Page intentionally left blank

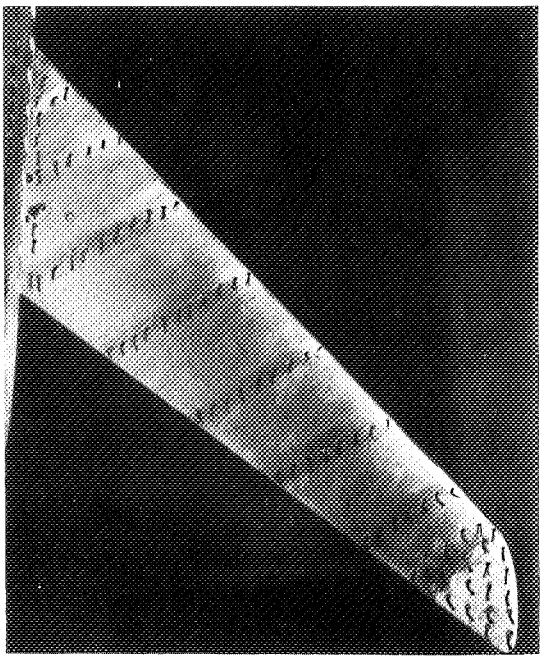

(e) $\alpha = 6^{\circ}$; upper surface; M = 0.80.

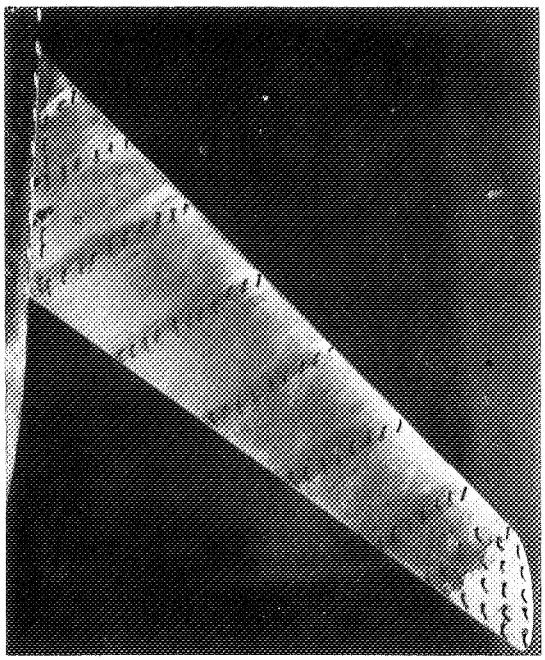

(f) $\alpha = 6^{\circ}$; upper surface; M = 0.89.

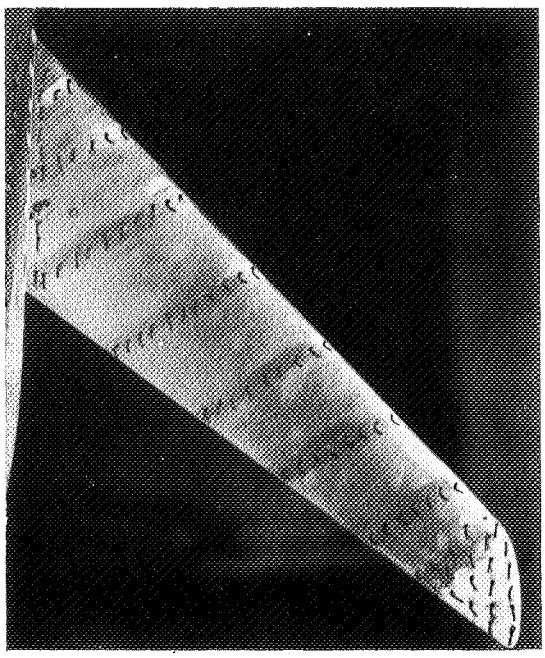

(g) $\alpha = 9^{\circ}$; upper surface; M = 0.60.

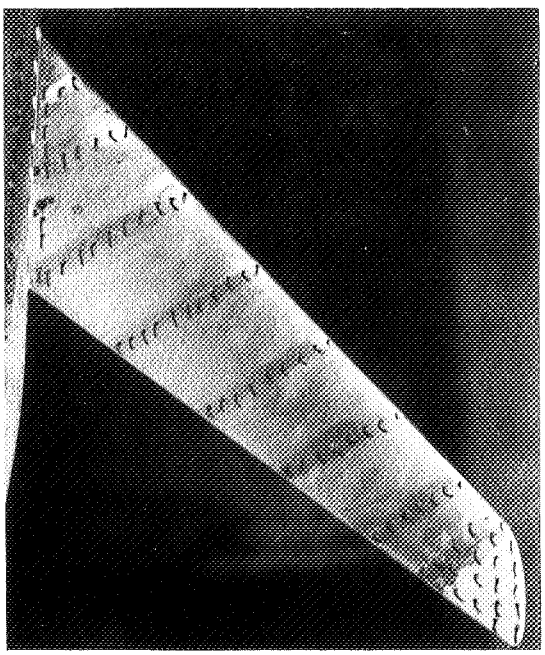

(h) $\alpha = 9^{\circ}$; upper surface; M = 0.80.

L-68400

Figure 11.- Concluded.

Page intentionally left blank

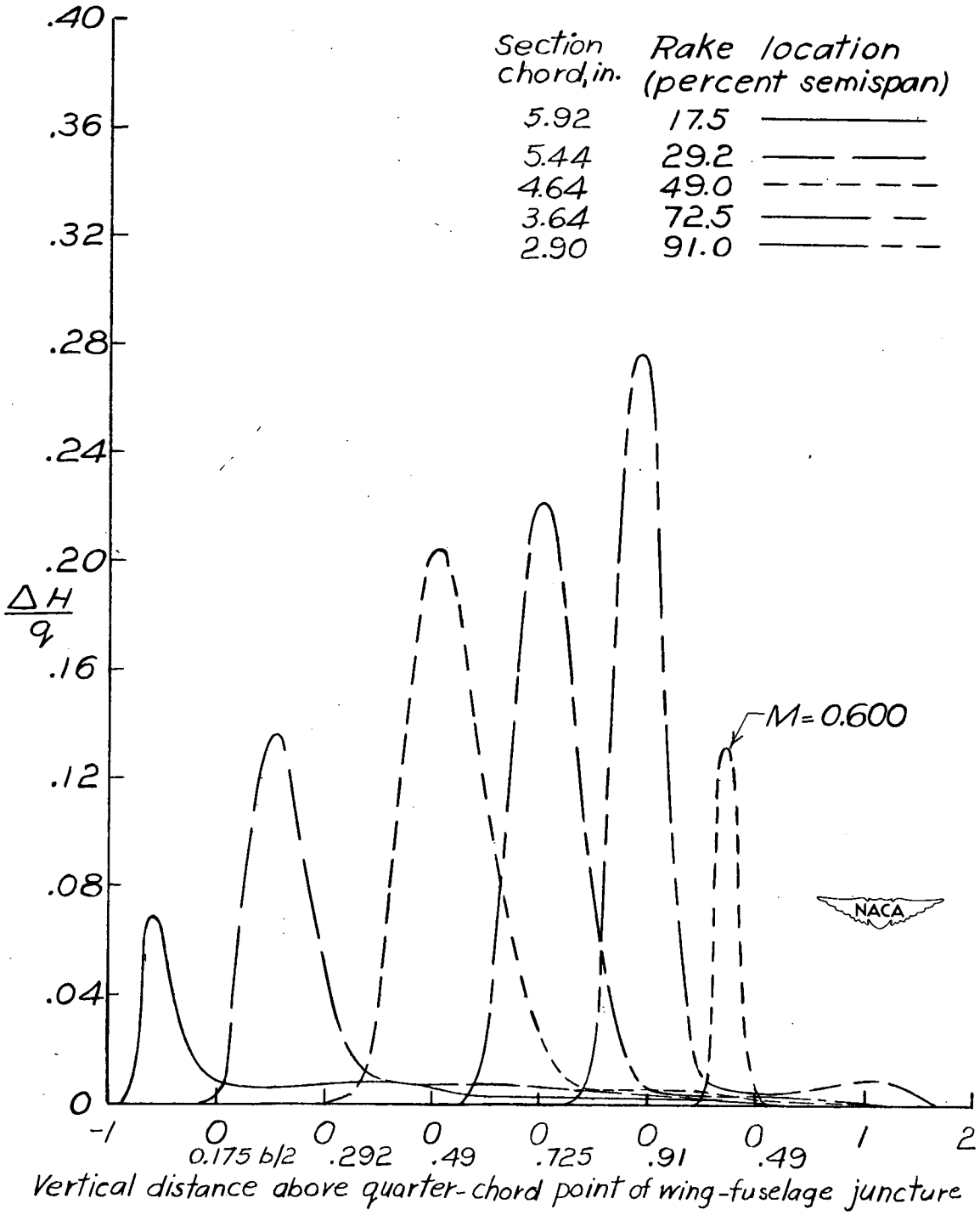

(a) $\alpha = 2^{\circ}$; $M = 0.890$.

Figure 12.- Wake profiles at various spanwise survey positions. $\Lambda = 30^{\circ}$.

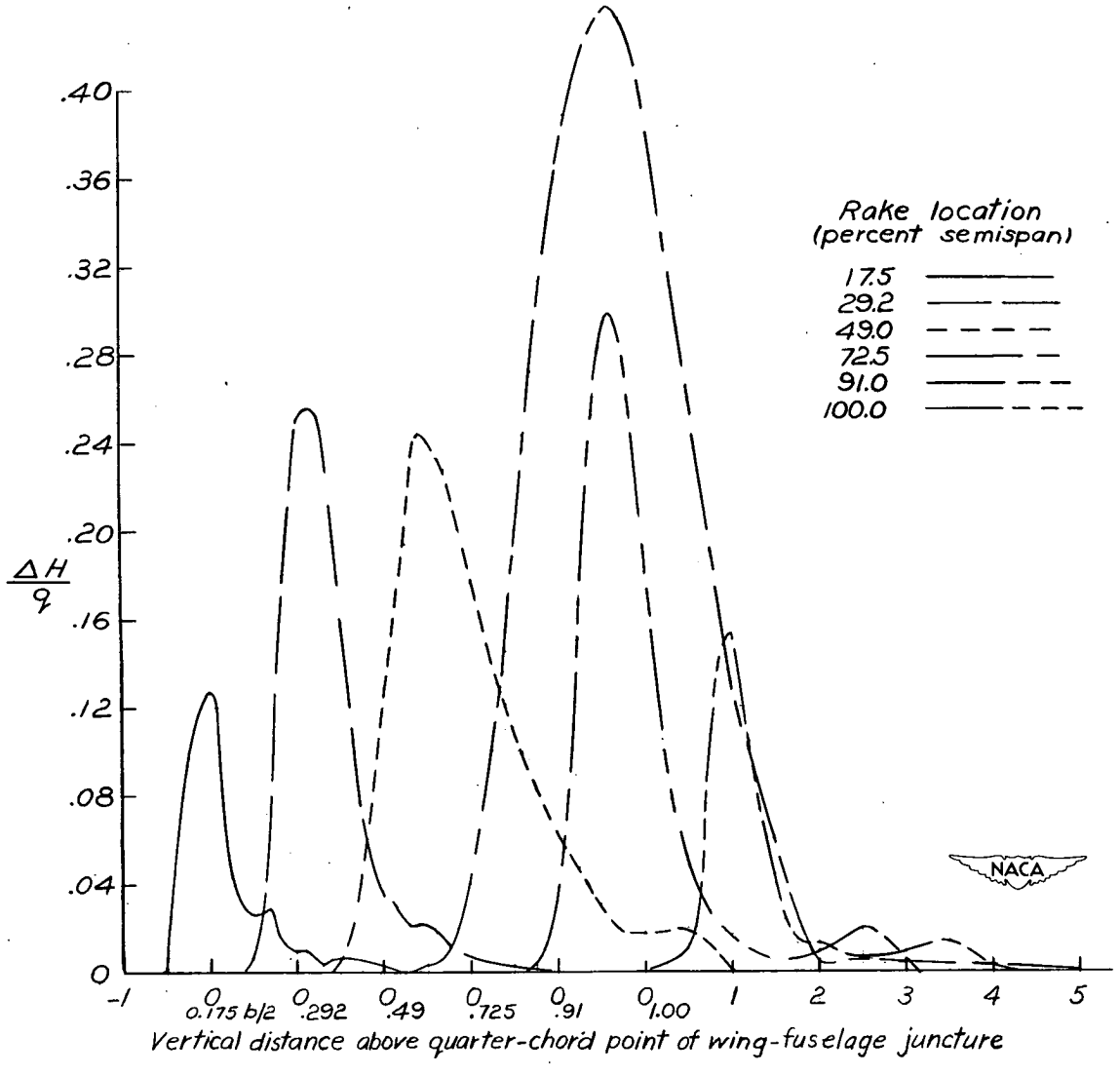

(b) $\alpha = 8^{\circ}$; $M = 0.80$.

Figure 12.- Concluded. $\Lambda = 30^{\circ}$.

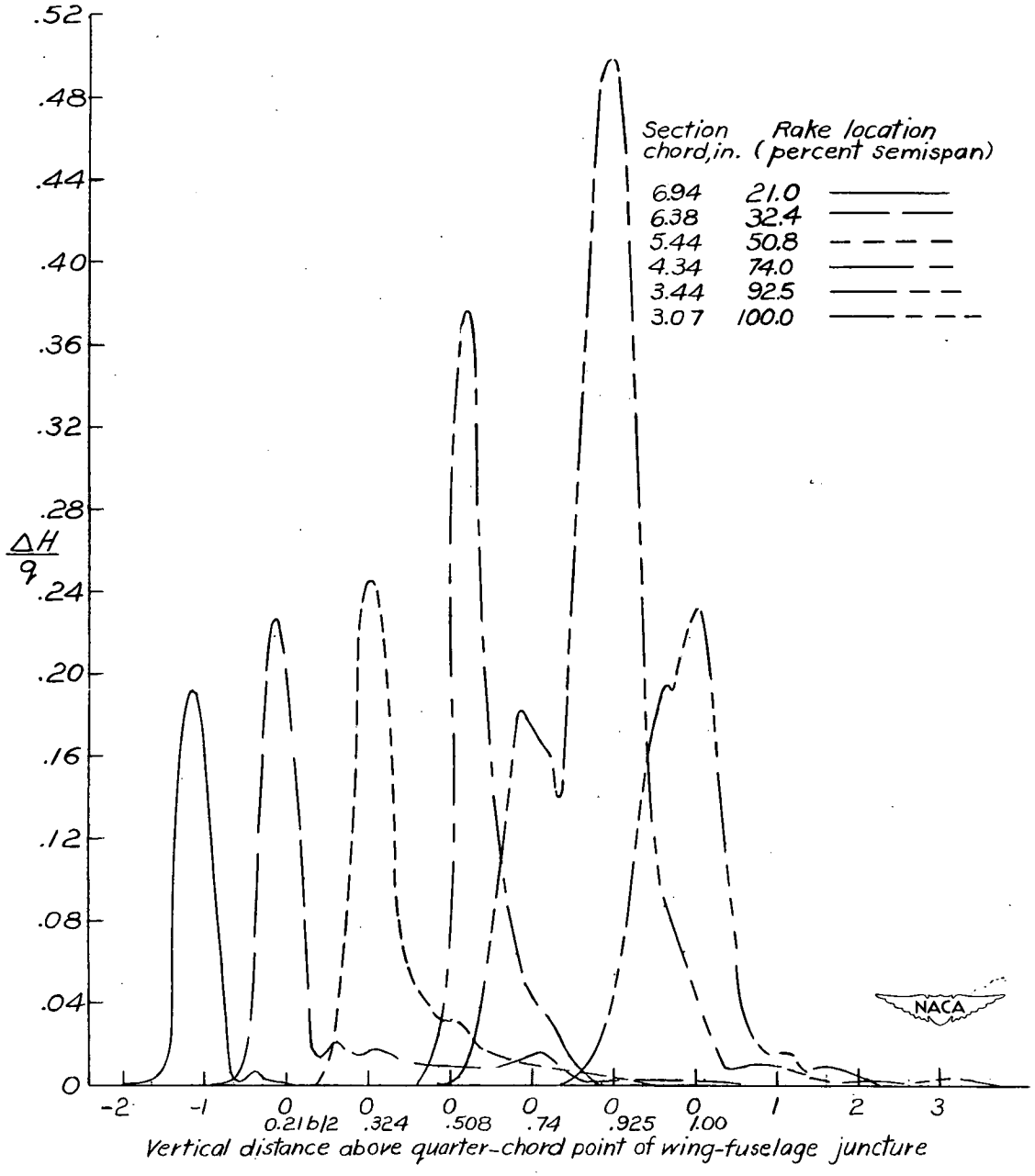

Figure 13.- Wake profiles at various spanwise vertical survey positions. $\Lambda = 45^{\circ}$; $\alpha = 6^{\circ}$; $M = 0.890$.

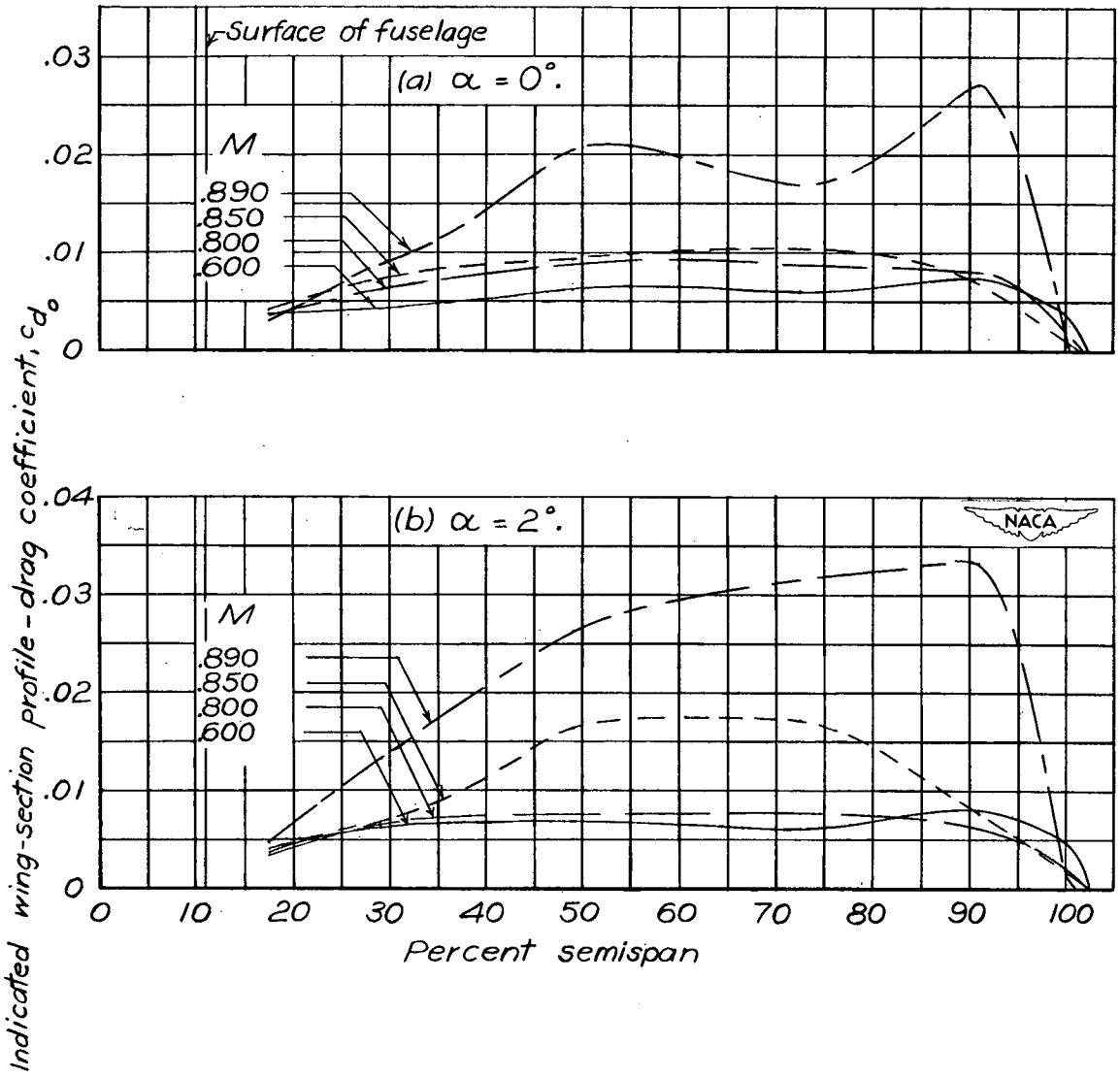

Figure 14.- Spanwise variations of indicated wing-section profile-drag coefficient for various Mach numbers. $\Lambda = 30^{\circ}$.

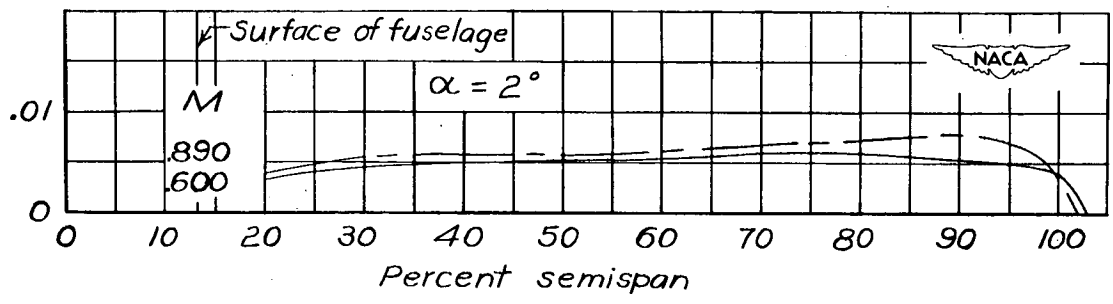

Figure 15.- Spanwise variations of indicated wing-section profile-drag coefficient for various Mach numbers. $\Lambda = 45^{\circ}$.

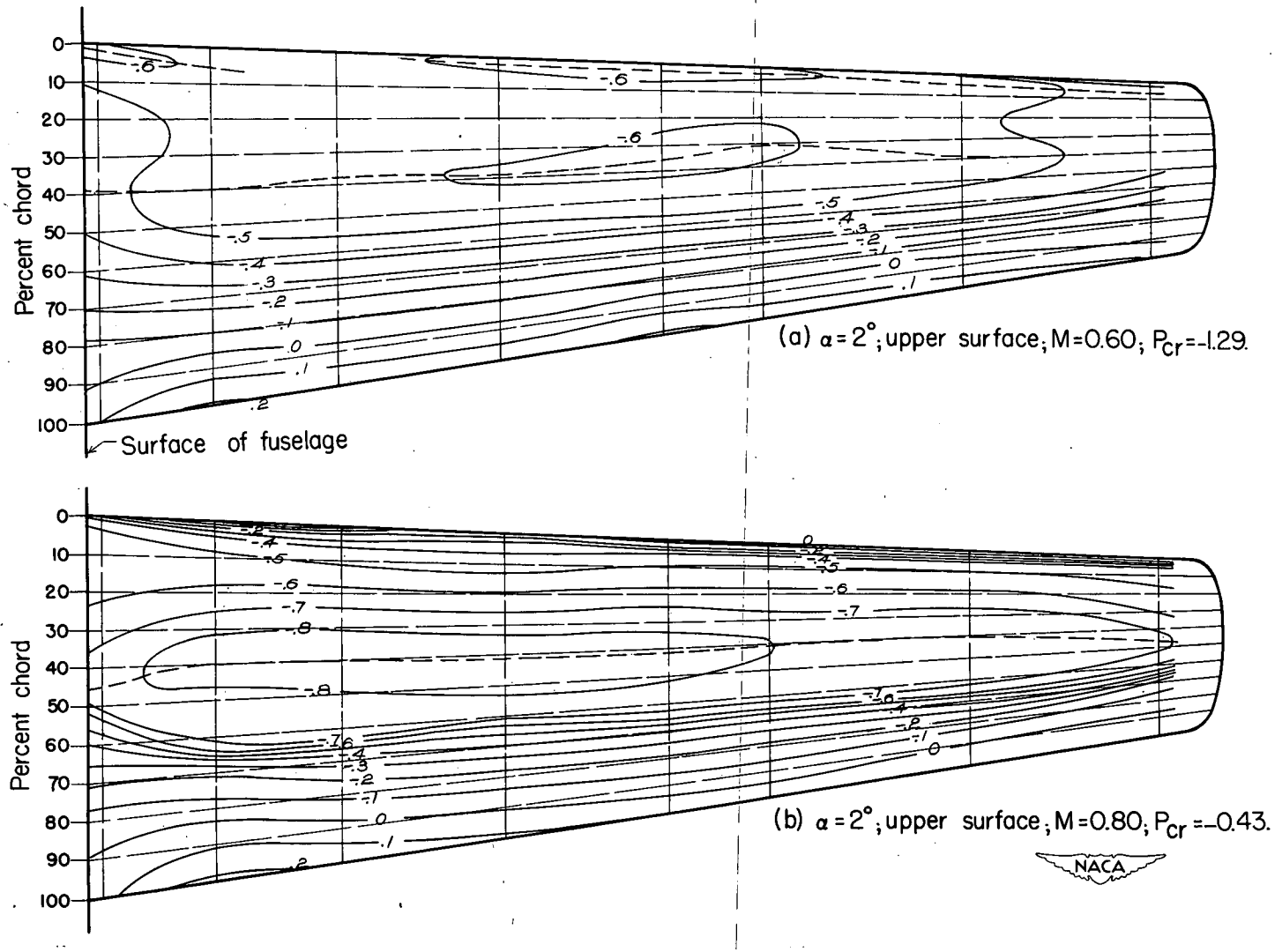

Figure 16.- Equal pressure-coefficient contours for comparable unswept wing.

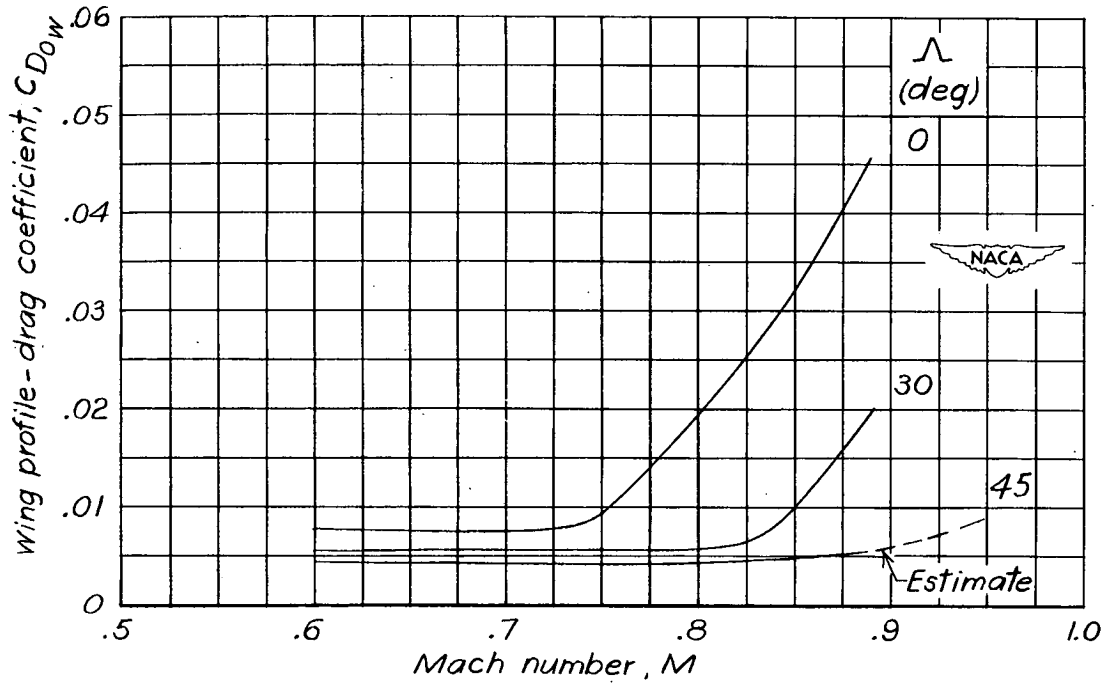

Figure 17.- Variations of wing profile-drag coefficients with Mach number. $\alpha = 2^{\circ}$.

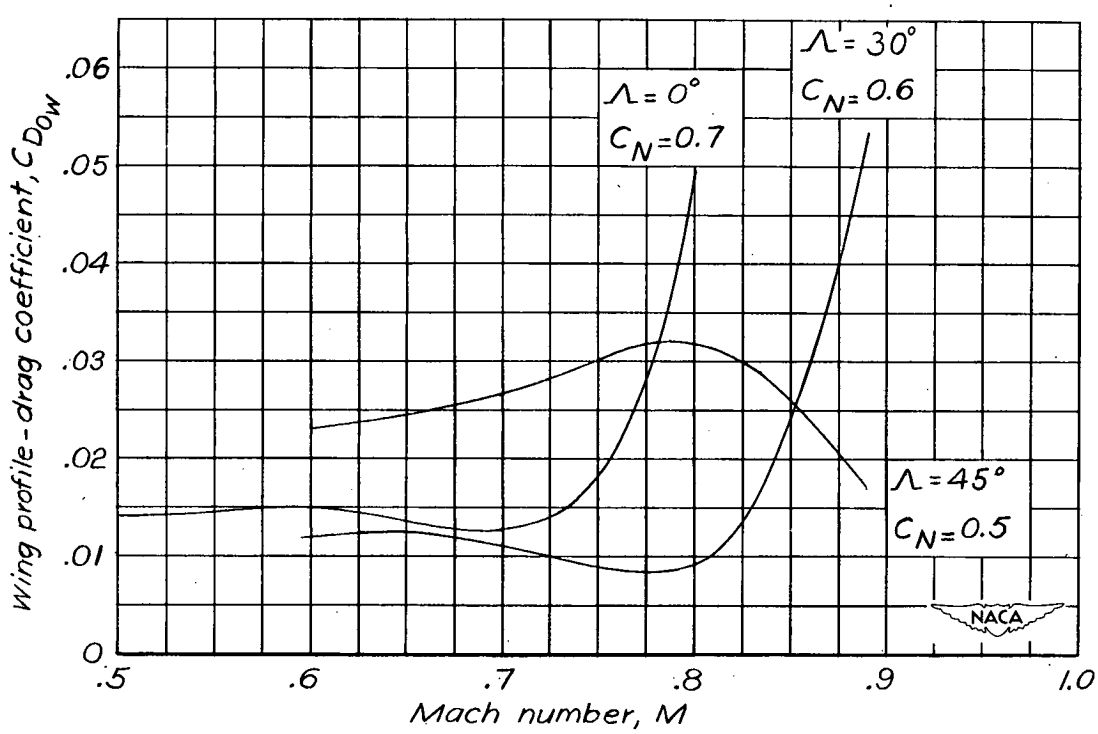

Figure 18.- Variations of wing profile-drag coefficients with Mach number at constant normal-force coefficients.